Development of Dehydroalanine Homo and Copolymers as Antibacterial Materials and Biocompatible Nanoparticle Coatings

by

YASEMİN YAR

A Thesis Submitted to the
Graduate School of Sciences and Engineering
in Partial Fulfillment of the Requirements for
the Degree of

Master of Science
in
Materials Science and Engineering

Koc University

October 2011

Koç University

Graduate School of Sciences and Engineering

This is to certify that I have examined this copy of a master's thesis by

Yasemin Yar

and have found that it is complete and satisfactory in all respects,
and that any and all revisions required by the final
examining committee have been made.

Committee Members:

_____

Havva Funda Yağcı Acar, Ph. D. (Advisor)

_____

Duygu Avcı Semiz, Ph. D.

_____

Uğur Ünal, Ph. D.

Date: _____

ABSTRACT

The research presented here focuses on the polymers of 2-acetamidoacrylic acid which is a captodative monomer, an amino acid derivative and a compound existing in natural antibiotics. Three important properties of this compound were investigated: reactivity in copolymerization with commercial monomers such as methacrylic acid and acrylonitrile, antimicrobial activity of its homo and copolymers and its applicability to quantum dots as a biocompatible coating.

The bacterial contamination is a great concern where polymeric materials are widely used such as medical devices, healthcare products, food packaging, textiles, etc. Therefore, last two decades have witnessed a significant increase in efforts to develop antibacterial polymers in order to overcome the microbial colonization. Research presented here investigates the antimicrobial potential of poly (2-acetamidoacrylic acid) and its copolymers with methacrylic acid (MAA) and acrylonitrile (AN). Both MAA and AN are widely used commercial monomers for a variety of applications from fibers to contact lenses. These copolymerizations provided the reactivity ratios between these monomers as well.

Quantum dots (QDs) have attracted tremendous attention as an emerging tool for biomedical applications. Even though quantum dots are still controversial due to their high cytotoxicity, they have tremendous potential as fluorescent probes for early detection of cancer and also for drug delivery. Research presented in this dissertation addresses the need for improvement of aqueous stability and cytotoxity of quantum dots along with improved luminescent properties. In order to achieve this goal, cysteine which is one of the most popular biocompatible coatings for QDs and 3-MPA (3-mercaptopropionic acid) which is probably the most used QD coating material was evaluated as a co-stabilizer in the CdS synthesis along with Poly(2-acetamidoacrylic acid).

ÖZET

Burada sunulan araştırma kaptodativ monomer, bir amino asit türevi ve doğal bir bileşik olan 2-asetamidoakrilik asitin polimerlerini konu almaktadır. Bu bileşiğin üç önemli özelliği incelenmiştir: metakrilik asit ve akrilonitril gibi ticari monomerler ile kopolimerizasyonundaki reaktivite oranı, homo ve kopolimerlerinin antibakteriyel aktivitesi ve biyo-uyumlu bir kaplama malzemesi olarak kuantum noktacıklarına uygulanabilirliği.

Bakteriyel konteminasyon polimerik malzemelerin yaygın olarak kullanıldığı tıbbi cihazlar, sağlık ürünleri, gıda ambalajı, tekstil ürünleri ve benzeri uygulamalarda büyük bir endişe kaynağı olmaktadır. Bu nedenle, mikrobiyel kolonizasyonun üstesinden gelebilmek için son yirmi yıl antibakteriyel polimerlerin geliştirilmesi konusunda büyük bir çabaya tanık olmuştur. Burada sunulan araştırmada poli(2-asetamidoakrilik asit) ve metakrilik asit (MAA) ve akrilonitril (AN) ile olan kopolimerlerinin antibakteriyel potensiyelini incelenmektedir. Bu polimerizasyonlar monomerler arasındaki reaktivite oranlarını da göstermektedir. Hem metakrilik asit hem akrilonitril yaygın ticari monomerler olarak fiberden kontak lense kadar çeşitli uygulamalar için kullanılmaktadırlar..

Kuantum notacıkları (QDs), biyomedikal uygulamalar için gelişmekte olan bir araç olarak büyük bir dikkat çekmiştir. Kuantum noktacıkları, halen yüksek hücre toksisiteleri nedeniyle tartışmalı olsa da, kanserin erken tespiti ve ilaç yönlendirmede muazzam bir potensiyele sahiptir. Bu tezdeki öncül hedef suda asılı kalan, iyi ışıyan ve biyo-uyumlu olan nano parçacıklar sentezlemektir. Bu hedefi mümkün kılmak için öncelikle sistin, biyo-uyumluluğu bilinen bir kaplama malzemesi, ve 3-MPA (3-mercaptanpropionik asit), kuantum noktacıklarını kaplamada en çok kullanılan malzeme, CdS sentezinde bir ko-stabilizatör olarak poli(2-asetamidoakrilik asit) ile birlikte değerlendirilmiştir.

ACKNOWLEDGEMENTS

Actually, it is very difficult to express my feelings in few words. First, I owe my deepest gratitude to my dear supervisor Assoc. Prof. Funda Yağcı Acar for her support and suggestions throughout my academic life at Koç University. With her enthusiasm and inspiration, she had motivated me all the time and showed the beauty of the world of the research. She could not even realize how much I have learned from her. When I gave up everything and I felt miserable, she always encouraged me, saying, "I trust you, you can do it." Without her invaluable guidance, I would have been lost.

I am deeply indebted to Prof. Burak Erman for expressing sincere care and concern toward me. He showed me at least some of the professors are aware of students can also have problems and grades are not more important from their well-being. I would like to acknowledge Prof. Duygu Avcı Temiz and Asst. Prof. Uğur Ünal for taking part in my thesis committee. I would like to also thank Asst. Prof. Özgür Birer for his interest and valuable discussions on my research. I would like to thank Dr. Gülen Ulusoy for her valuable contributions on the antibacterial testing and toxicology studies.

I am indebted to many of my colleagues, especially members of Polymers and Nanomaterials research team Hande Öztürk, Ceren Yılmaz, Sinem Ertaş, Hilal Çomak and Didar Aşık for their friendship, support and every laughter that brightened the days in which nothing went right. I am afraid that I will never find the chance to be a part of such a group. I will miss our talks during the tea times. My special gratitude goes to Didar Aşık. The results presented in here cannot be possible without the hard work of Didar. Without any doubts, she was so altruistic that she worked with me till mornings and gave up her holiday because of me. I would thank Selçuk Acar for helping me with TGA measurements. I greatly appreciate his valuable time. Also, I have to thank Muharrem Güler for his help about all lab equipment.

Above all, I want to give the most special thanks to my parents for their incredible mental support. Thank you for your understanding and the courage you have given me. Finally I want to express my deep gratitude to Taner Ruşen for his love, support and patience that has been never ended.

TABLE OF CONTENTS

LIST OF TABLES

LIST OF FIGURES

NOMENCLATURE

AAA	2-Acetamidoacrylic acid
ACVA	4,4'-Azobis-4-cyanovaleric acid
AIBN	2,2'-Azobisisobutyronitrile
AN	Acrylonitrile
ATR	Attenuated Total Reflectance
B.subtilis	*Bacillus subtilis*
CD	Captodative
CFU	Colony-Forming Units
CMF-PBS	Ca^{2+}, Mg^{2+} Free Phosphate Buffered Saline
DHA	Dehydroalanine
DMEM	Dulbecco's Modified Eagle Medium
DMF	Dimethylformamide
DMSO	Dimethylsulfoxide
DSC	Differential Scanning Calorimetry
e	Polar Factor of Monomer
EBR	Exciton Bohr Radius
E.coli	*Escherichia coli*
f	Initiator Efficiency
FBS	Fetal Bovine Serum
FT-IR	Fourier Transformed Infra-Red
FWHM	Full Width At Half Maximum
GPC	Gel Permeation Chromatography
^{1}NMR	Proton Nuclear Magnetic Resonance
k_d	Rate Constant of Radical Decomposition
k_p	Rate Constant of Propagation

k_t	Rate Constant of Termination
LB	Lysogeny Broth
m-AATBTB	*m*-acryloylamino-(tri-*n*-butyltinbenzoate)
MAA	Methacrylic Acid
3-MPA	3-Mercaptopropionic Acid
N-TBTM	*N*-tri-*n*-butyltin)maleimide
OD	Optical Density
Q	Resonance Factor of Monomer
QDs	Quantum Dots
Quats	Quaternary Ammonium Salts
P(AAA)	Poly(2-acetamidoacrylic Acid)
PAN	Poly(acrylonitrile)
PDMEMA	Poly(2-dimethylaminoethyl)methacrylate
PDI	Polydispersity Index
PL	Photoluminescence
RCS	Refrigerated Cooling System
r	Reactivity Ratio
TGA	Thermogravimetric Analysis
THF	Tetrahydrofuran
UV-Vis	Ultraviolet-Visible-Near Infrared
v	Kinetic Chain Length of A Polymer
[I]	Initiator Concentration
[M]	Monomer Concentration

Chapter 1

INTRODUCTION

1.1 The Concept of Captodative Effect

Free radical polymerization is the most widely used method of polymerization because of high reproducibility, adaptability to many types of monomers, solvents, and simple experimental conditions.[1] However, a radical is a short-lived, highly reactive species. Therefore, controlling a free radical reaction is not that easy. Recently, different methods have been developed to control the stability of radicals formed in a free radical polymerization, i.e. chemical and physical regulation.[1] Although substituent effects in free radical polymerization have attracted tremendous attention, the *captodative (cd) effect* which is also known as the *push-pull stabilization*, the geminal substitution of an electron-withdrawing (Latin 'captare') and electron-donating (dative, Latin 'dare') groups on the same radical center, has not received considerable attention up to now, and it has not been studied systematically in the fields of organic and polymer chemistry yet.[2,3] The *cd* effect was postulated on the basis of the assumption that a radical might be stabilized by synergistic effect of both an electron-donor and –acceptor groups, whereas a carbocation is stabilized by electron donating substituents and a carbanion is stabilized by electron accepting substituents (Figure 1.1).[3] Because of the presence of the experimental and/or theoretical errors, the validity of *cd* effect was debated until about twenty years ago and most of the free radical polymer chemists denied this concept.[3] At present, the *cd* effect has found acceptance and it is known that the *cd* radicals are stabilized thermodynamically when and because additional resonance stabilization can occur

wherein the unpaired, odd electron is delocalized onto the electron donor and acceptor groups.[3,4] In other words, *cd* effect gives extra stabilization to radical and this situation not only plays important roles in the stability but also affects reactivity of the formed *cd* radical. [3,4]

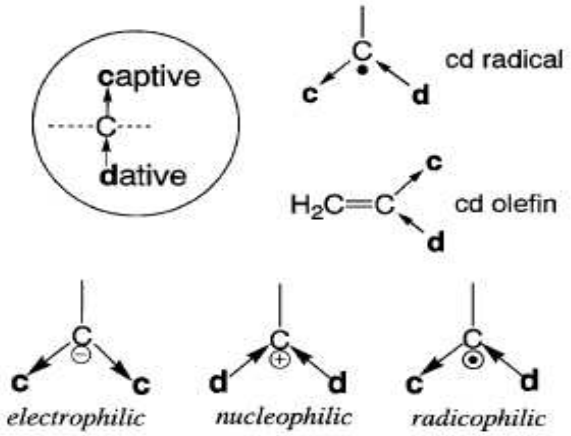

Figure 1.1 Captodative substitution.[3]

1.1.1 Dehydroalanines

The presence of α-amino acrylic acid (dehydroalanine) in proteins was reported firstly in 1945 by Cuthbertson and Phillips.[5] Dehydroalanine (DHA) is an uncommon amino acid that is present in a variety of naturally occurring peptide antibiotics of bacterial origin, including "lantibiotics" nisin, subtilin, epidermin, gallidermin.[6,7] Lantibiotics are defined as the class of antibiotic polycyclic peptides that contain the rare thioether amino acids lanthionine or methyllanthionine and also have DHA and/or dehydrobutyrine residues.[6,8] The most well-known lantibiotics are nisin and subtilin which are used as natural food preservatives in industry. Nisin and subtilin do not pose health hazards to humans. In addition, they do not give harm the bacteria of intestinal flora so they are given preference over nitrates and nitrites in food industry, which threaten human health with cancer risk.[8]

The presence of DHA units in peptides plays important roles in biological activities.[8,9] For instance, the existence of DHA in a synthesized peptide acts as an inhibitor of spider venom.[8,9] Besides, the presence of DHA residues in nisin and

subtilin are responsible for the inhibition of outgrowth of bacterial spores.[8,9] Interestingly, it was found that the role of DHA is crucial in the anti-bacterial activity. The absence of DHA caused a dramatic decrease in the nisin's ability to inhibit the bacterial growth.[8]

Dehydroalanine (DHA) derivatives, which are examples to *cd* olefins, have been reported to undergo facile polymerization under free radical conditions that gives polymers in high yield with very high molecular weight.[10-13] This situation is attributed to the captodative stabilization effect (Figure 1.2). It should be noted that not all *cd* radicals are highly stabilized because total stabilization depends on the magnitude of the stabilization of the individual capto and dative groups. The most crucial drawback of free radical polymerization is the effect of steric hindrance.[3,4] However, poor polymerizability of 1,1-disubstituted monomers can be overcome by choosing appropriate *cd* substituted molecules.[3] Therefore, polymerizability depends on the nature of the donor and acceptor groups. An important property of the polymerizable *cd* olefins is that some of these olefins can display spontaneous polymerization even in the absence of an initiator.[2] This fact can be understood by considering the ease of formation of the initiating radical species.

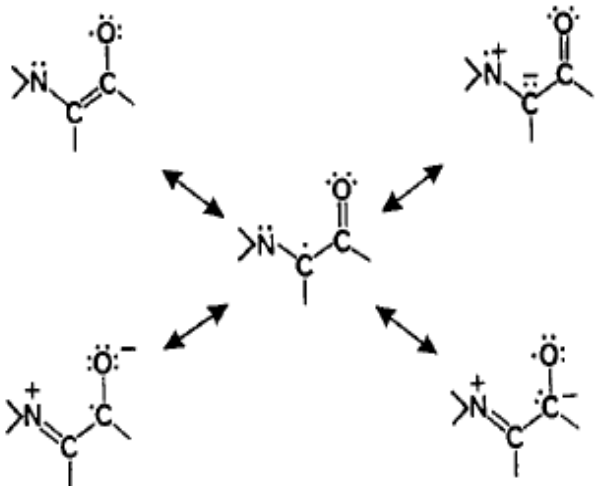

Figure 1.2 Resonance stabilization due to captodative effect.

It is important to realize that polymerization of a monomer not only depends on the rate constant of propagation but also depends on the rate constant of

termination so that *cd* stabilization of the propagating radical can't be undertaken as a preventing factor for polymer formation.[13]

1.1.2 Polymerization of Dehydroalanines

Interestingly enough, not much research is done on the polymerization and copolymerization of dehydroalanines. The most important reason for that is the free amino acid monomer can not be isolated because of the spontaneous decomposition to ammonia and pyruvic acid. Since N-acetyl derivative of dehydroalanine (AAA) is stable, earlier works deal with the N-acetyl dehydroalanine (2-acetamidoacrylic acid), and reports utility in various application areas such as metal complexation, hair treatment, and quantum dot stabilization in a hydrogel.[14,15] However, these reports do not usually provide detailed information on polymer properties or compositions. Literature provides some preliminary information on the kinetics of 2-acetamidoacrylic acid (AAA) in dimethylsulfoxide (DMSO) and copolymerization with styrene.[14]

Although there are only very few, 2-acetamidoacrylic acid demonstrates a large reactivity difference when copolymerized with common acrylics such as acrylic acid.[14] Copolymer composition is generally different than the composition of the comonomer feed. The tendency for copolymerization of monomers is denoted by *r* (reactivity ratio) which is the ratio of the rate constant for a reactive propagating radical adding to its own type of monomer to the rate constant for its addition to the other monomer. When $\sim\sim\sim\sim M_1^{\cdot}$ prefers to add the monomer M_1 instead of monomer M_2, the monomer reactivity ratio,r_1 value is greater than unity., while an r_1 value less than unity means that $\sim\sim\sim\sim M_1^{\cdot}$ prefers to add the monomer M_2.

The information on reactivity ratios for monomer pairs is very important in adjusting copolymer composition and properties. Monomer reactivity ratio depends on the parameter Q, which describes the resonance factor present in the monomer, and the parameter e, which describes the polar factor. In the polymerization of 2-acetamidoacrylic acid (M_1) with styrene in DMSO, r_1 and r_2 was determined as 0.53 and 0.11, and the Q and e values were calculated as 2.43 and 0.89, respectively for 2-acetamidoacrylic acid.[14] 2-acetamidoacrylic acid is an acetylamido derivative of

acrylic acid. In the literature, it has been reported that for acrylic acid (M_2) Q = 0.83 and e = 0.88.[14] Although there is almost no difference between e values, Q value of 2-acetamidoacrylic acid is significantly greater than that of acrylic acid.

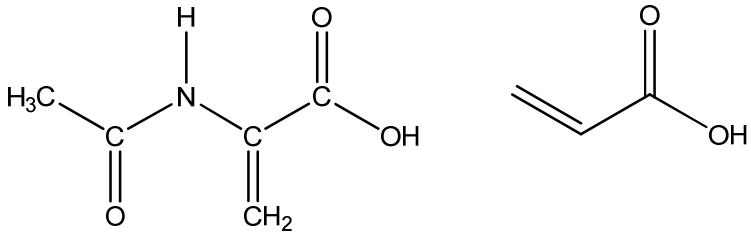

2-Acetamidoacrylic Acid (M_1) e = 0.89

Acrylic acid (M_2) e = 0.88

Figure 1.3 Q and e values of 2-acetamidoacrylic acid and acrylic acid.[14]

More recent literature focuses on the homopolymerization of methyl ester of 2-acetamidoacrylic acid (M_3) in organic solvents and the copolymerization with acrylic acid, styrene (M_4) and other monomers.[16] Parameters r_3=3.04, Q_3=6.03, e_3=0.52 were determined where r_4=0.058, Q_4= 1.0 and e_4= -0.80 from the copolymerization of α-Acetylaminoacrylate and styrene at 50°C in tetrahydrofuran with AIBN as the initiator.[16] α-Acetylaminoacrylate is an acetylamino derivative of methyl acrylate. As in the case of 2-acetamidoacrylic acid and acrylic acid there is hardly any difference between e values of α-acetylaminoacrylate and methyl acrylate (M_5). Similarly, the Q value of α-acetylaminoacrylate is significantly greater than that of methyl acrylate.

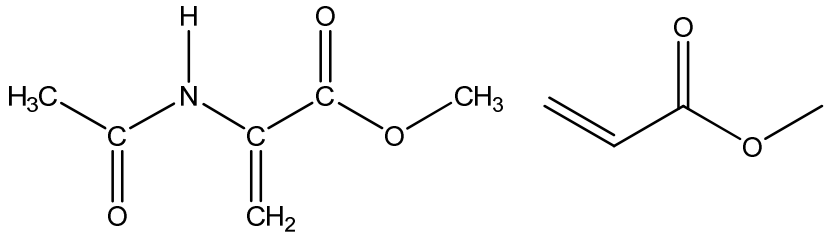

α-Acetylaminoacrylate (M_3) Q = 6.03 e = 0.52

Methyl Acrylate (M_5) Q = 0.45 e = 0.64

Figure 1.4 Q and e values of α-acetylaminoacrylate and methyl acrylate.[16]

Almost the same e values can be considered as acetylamino group has no contribution on the polarizing effect of monomer, meaning that electron density on the vinyl group is not affected by the presence of acetylamino group.[16] However, interestingly and considerably greater Q values can be attributed to the conjugation of carbon-carbon double bond with carbonyl group of the acetyl through lone-pair electrons on nitrogen atom which gives rise to resonance stabilization.[16] The large Q values of these monomers indicate that the propagating radical is highly stabilized by the resonance and the resonance factor of the monomer determines the magnitude of monomer reactivity, moreover it is more important than the polar factor.[16]

1.2 Antimicrobial Polymers

The bacterial contamination is a great concern where polymeric materials are widely used in such as medical devices, healthcare products, food packaging, textiles, etc. For instances, bacterial contamination of permanent catheters or implants can cause severe complications. Undoubtedly, it is very apparent that there is a need for new materials which are capable of killing pathogenic microorganisms. Therefore, last two decades have witnessed a significant increase in efforts to synthesize and develop antibacterial polymers in order to overcome the microbial colonization. There are various kinds of methods to achieve antimicrobial polymers such as:

1) addition of low molecular weight antimicrobial agents
2) use of functional monomers bearing groups with antimicrobial activity
3) incorporation of known biocidal groups like quaternary ammonium salts

1.2.1 Addition of Low Molecular Weight Antimicrobial Agents

One method of obtaining antimicrobial polymers is to add organic or inorganic antimicrobial agents to the polymers during processing. Triclosan (2, 4, 4'-trichloro-2'-hydroxydiphenyl ether), a chlorinated phenoxy phenol compound, is a common ingredient of number of consumer products such as detergents, soaps, deodorants, cosmetics because it is a non-specific biocide meaning that it kills all

types of microbes. However, the use of low molecular weight biocides such as Triclosan has been questioned in regard to environmental and human health.

1.2.2 Use of Monomers Bearing Groups with Antimicrobial Activity

Another method of achieving antimicrobial polymers is to synthesize polymers from monomers with antimicrobial moieties. The antimicrobial activity of the prepared polymers is either reduced or enhanced by polymerization.

Al-Diab and coworkers synthesized two novel organotin monomers: (*N*-tri-*n*-butyltin)maleimide (N-TBTM) and *m*-acryloylamino-(tri-*n*-butyltinbenzoate) (m-AATBTB) (Figure 1.5).[17] The copolymerization of these monomers with styrene at 65°C was carried out in bulk with AIBN, the antimicrobial activity of resulting copolymers and monomers were tested against various types of Gram-positive and Gram-negative bacteria after 24 hour contact time. Results showed that the polymerization of organotin monomers decreased the antimicrobial activities significantly. This is simply a result of decreased amount of tin-complex per gram of sample as in the polymer there is a significant amount of styrene as well which has no antimicrobial activity.[17]

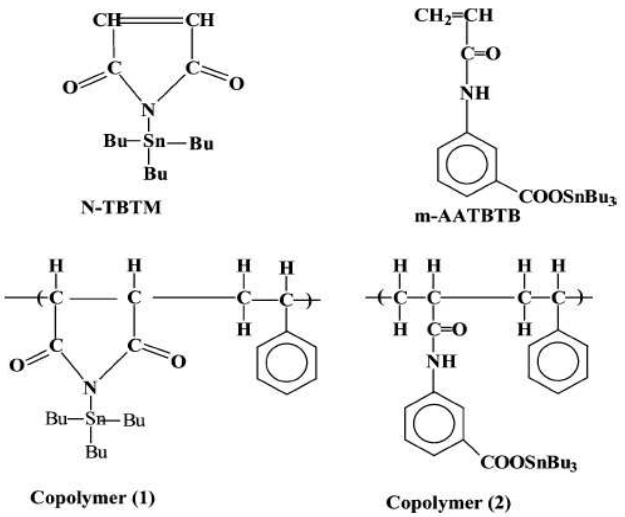

Figure 1.5 Monomers and copolymers based on N-TBTM and m-TBTM.[17]

On the contrary, in some cases the polymerization of monomers with antimicrobial moieties can enhance the antimicrobial activity. Polymerization of 2-hydroxy-3-(5-methyl-1,3,4-thiadiazol-2-yl)thiopropyl methacrylate increased the potency of biocidal activity.[18] There are no data reporting the mode of actions of this monomer or its polymer; however, they may function as benzimidazole derivatives, which are proposed to inhibit the cytochrome P-450 monooxygenase.[18]

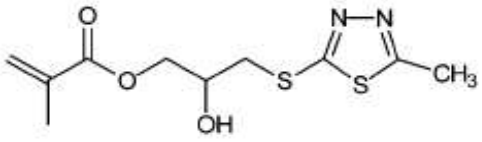

Figure 1.6 2-hydroxy-3-(5-methyl-1,3,4-thiadiazol-2-yl)thiopropyl methacrylate.[18]

1.2.3 Incorporation of Quaternary Ammonium Salts

Polymers with antimicrobial activity can be prepared via alkylation of tertiary amine, in a process called quaternization. Quaternary ammonium compounds are basically cationic surfactants that have a hydrophilic head and hydrophobic tail. Therefore, they are used in formulations of cleansers for hard-surfaces and in disinfectants for water-resistant surfaces. Quaternary ammonium salts, also known as quats or polyquats in the case of polymeric cationic structures, the most widely used antimicrobial agents. Quats are believed to be adsorbed on the negatively charged cell surface of bacteria and penetrate through the membrane, changing permeability of plasma membrane, which leads to cellular leakage and cell death.

1.3 Quantum Dots

Fluorescent semiconductor nanoparticles or quantum dots (QDs), are spherical nanometer-sized crystals made of II-VI (i.e. CdS, CdTe and ZnSe), III-V (i.e. GaAs, InP) or IV-VI (i.e. PbS, SnTe) main group elements of periodic table and exhibit, unique properties different from the corresponding bulk materials. Normally, the size

of the QDs is between 1-100 nm, but according to some literature the diameter of QD should be strictly smaller than 10 nm.[19] At such reduced sizes, these particles behave differently from bulk materials which provides unique properties with potential applications.

1.4 Energy Bands and Bandgaps

In a bulk semiconductor, energy levels of electrons are so close to each other that they are described as continuous which means there is almost no energy difference between them. Because quantum dots are semiconductor materials and just like any semiconductor, some energy levels are forbidden so that the conductivity of a semiconductor depends on the *band gap*. The band gap is defined as the energy difference (in electron volts) between the valence and the conduction band and it is different for each bulk material (Figure 1.7). Energy states above the band gap is called the conduction band which is unoccupied by electrons. The energy states lying below the band gap is called the valence band which is fully occupied by the valence electrons.

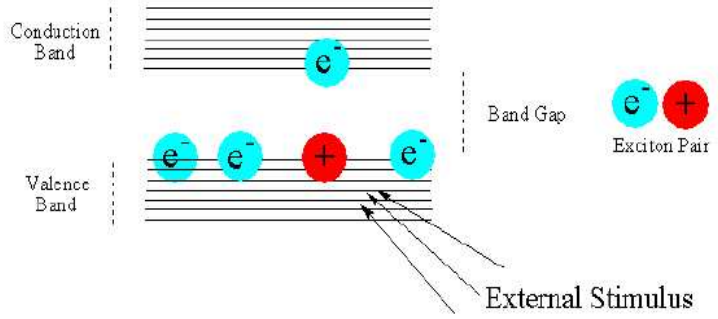

Figure 1.7 Creation of Exciton in a Semiconductor (www.evidenttech.com).

If an incident photon having certain energy is given to quantum dots, an electron in the ground state is excited to higher energy levels leaving a hole behind and this process is called as absorption of light. This electron-hole pair is called *exciton* and the distance between electon-hole pair is defined as *Exciton Bohr Radius (EBR)*.

When the size of a semiconductor crystal is as small as the EBR, *quantum confinement effect* occurs, meaning that the energy states are quantized and no longer continuous. If the confinement appears to be in three dimensions, these tiny semiconductor crystals are called as *quantum dots*. Forcing exciton pair to occupy a space smaller than the normal equilibrium distance in the bulk material (dotted line) causes to take more energy to promote the electron from the valance band to the conduction band, as a result of such confinement band gap of the QD is always larger than the band gap of its bulk form (Figure 1.8). Moreover, the smaller the size of QD, the larger the band gap of the material.

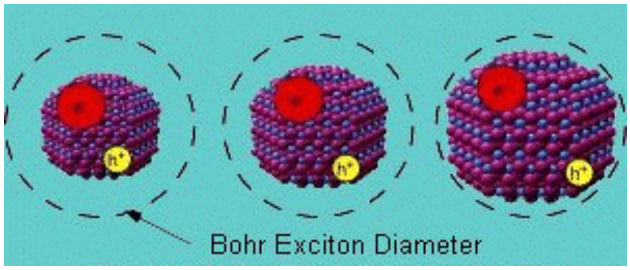

Figure 1.8 Quantum confinement effect (www.vanderbilt.com).

1.5 Size Tunable Optical Properties

What make quantum dots so interesting are the size tunable optical and electronic properties due to the quantum confinement effect.

Since in a bulk semiconductor the band gap is fixed and the energy states are continuous the absorption spectrum of a bulk semiconductor is uniform. However, in the case of QDs the absorption is discontinuous. The wavelength at which discontinuity starts is called *absorption edge (onset)* and the peak seen in the absorption spectrum corresponds to the optical transitions between the electron and hole levels (Figure 1.9). It is also referred as the minimum energy and thus the maximum wavelength peak corresponds to the first exciton peak or the energy for an electron to jump from the highest valence state to the lowest conduction state. Larger quantum dots have an absorption edge that is shifted to longer wavelengths with respect to smaller quantum dots.

However, the excited electron has a tendency to relax back to its original position, ground state since the excited state is not stable. The relaxation can occur as either a non-radiative or a radiative event. Non-radiative decay occurs through the loss of heat via lattice vibrations. Radiative decay occurs when the recombination of the electron with the hole leads to the generation of a photon. If the photon energy is within 1.8 eV to 3.1 eV, an energy loss by the emission of photons is in the visible range, a phenomenon called *fluorescence*.[20] As the size of QDs gets smaller, light absorption and emission occurs at a shorter wavelength as the band gap increases. In Figure 1.10, the color of emitted light is represented on the dots with size change.

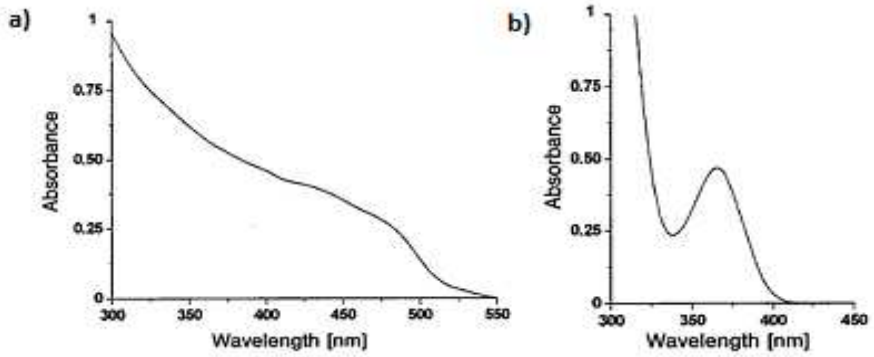

Figure 1.9 UV-vis spectra of (a) bulk CdS and (b) 4 nm CdS (http://cnx.org).

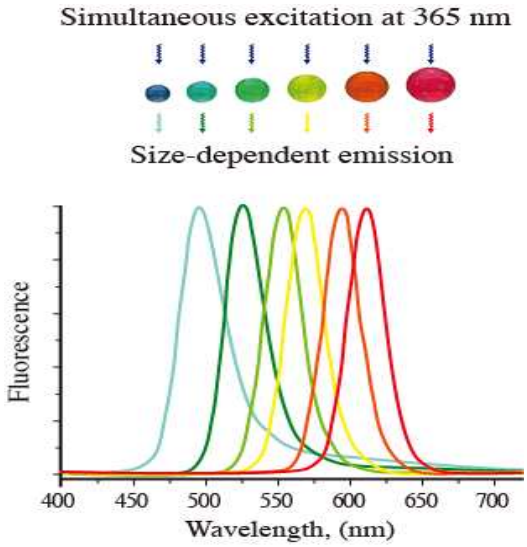

Figure 1.10 Fluorescence spectra depending on the size of the quantum dots (http://www.aist.go.jp).

Since some of the energy is lost due to the non-radiative relaxation path ways of the excited electron, the energy of the emitted photon through the radiative decay is smaller than the absorbed energy. Therefore, the emission wavelength is longer than the absorption onset or the wavelength of absorbed light. This difference is called as the *Stoke's Shift* (Figure 1.11).

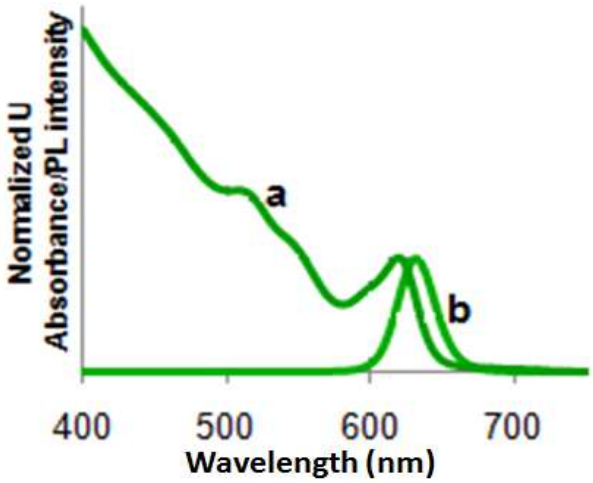

Figure 1.11 Absorption spectra (a) and emission spectra (b) of CdSe tetrapod (http://cnx.org).

1.6 Medical Applications of Quantum Dots

Quantum dots have garnered much attention as an emerging tool for biomedical applications. Unfortunately, cancer has become the major cause of death in all over the world. There is an increasing demand for early detection and "cure" for cancer. Early detection and effective treatment is the most crucial thing to avoid death for cancer patients hence, there is a need to develop cancer-specific imaging probes for the early diagnosis of cancer. However, cells are transparent to visible light so it is impossible to observe them with conventional microscope. Therefore, to overcome this challenge and make imaging a simpler task labeling the cells with a fluorophore will enhance the contrast. The use of conventional fluorophores is limited by their narrow absorption range, broad emission spectra, poor stability and short fluorescence

lifetime.[20] While organic fluorophores suffer from these reasons, quantum dots offer high photostability, narrow size tunable emission spectra, and broad absorption spectra. Even though quantum dots are still controversial due to their high cytotoxicity, they have tremendous potential as fluorescent probes for early detection of cancer and also for drug delivery.

Originally, the majority of the quantum dots were prepared in organic solvents, which means they can not be directly dispersed in physiological media. An aqueous approach, on the other hand, is needed to provide dispersion in physiological media. This is achieved through utilization of water soluble coatings which provides colloidal stability and protection for the crystal surface. Usually, hydrophilic polymers or small molecules with functional groups such as –COOH,-NH_2 or –SH are used as capping (coating) agent. Thiols strongly bind to Cd surface but COOH and amine groups can also stabilize CdX (X= S, Se, Te) particles. At least bifunctional materials are needed since one side provides binding to the crystal surface and the other interacts with water or the physiological medium to keep particles suspended.

Most widely used and studied QDs consist of cadmium selenide, telluride or sulfide.[20] Although CdX are promising fluorophores, toxicity is an important issue. The primary reason of cytotoxity is the release of cadmium ions which bind to thiol groups on critical molecules in mitochondria and induce harm and damage, causing significant cell death.[20] However, the release of Cd^{2+} ions can be controlled or reduced by effective surface passivization.[20] Also, coating molecule should not cause any toxicity either. Therefore, effective coating of the crystal surface and the selection of an appropriate coating material is crucial for physical, chemical and biological properties of QDs. Since surface functionalization plays the key role in nanoparticle stability and toxicity, if these problems could be solved, one day QDs can be safely used as a fluorescent probes for biological imaging and targeted delivery.

Chapter 2

DEVELOPMENT OF NOVEL COPOLYMERS OF 2-ACETAMIDOACRYLIC ACID AND INVESTIGATION OF THEIR ANTIBACTERIAL PROPERTIES

Research presented in this dissertation addresses the need for more information on the evaluation of capto-dative monomers as comonomers with traditional vinyl monomers such as methacrylic acid (MAA) and acrylonitrile (AN). Both MAA and AN are widely used commercial monomers for a variety of applications from fibers to contact lenses. For instances, copolymerization of AAA monomer with AN is important since AN-based copolymers are used widely in the production of fibers, used in the manufacture of blankets, carpets and clothing such as sweaters, socks, sportswear. In addition, they have uses in aerospace and aeronautical sectors as reinforcement for structural composites. The major drawbacks of the Poly(acrylonitrile) (PAN) fibers are poor hygroscopicity and low dye uptake. Since AAA is an acidic monomer it can not only improve the hygroscopicity of PAN fibers but also act as a promising comonomer which may introduce antibacterial properties to PAN. Therefore, ability to render these polymers antibacterial with the addition of Poly(dehydroalanine) derivative is very attractive scientifically and commercially. PMAA is used as dispersant, rheology controller, thickener in paint and printing industries, bath tubs and light weight shatter-proof synthetic glass alternative.Therefore,2-acetamidoacrylic acid was copolymerized with methacrylic acid and acrylonitrile, reactivity ratios of the monomers were calculated, compositions of the copolymers were determined, and antibacterial properties of these polymers were investigated.

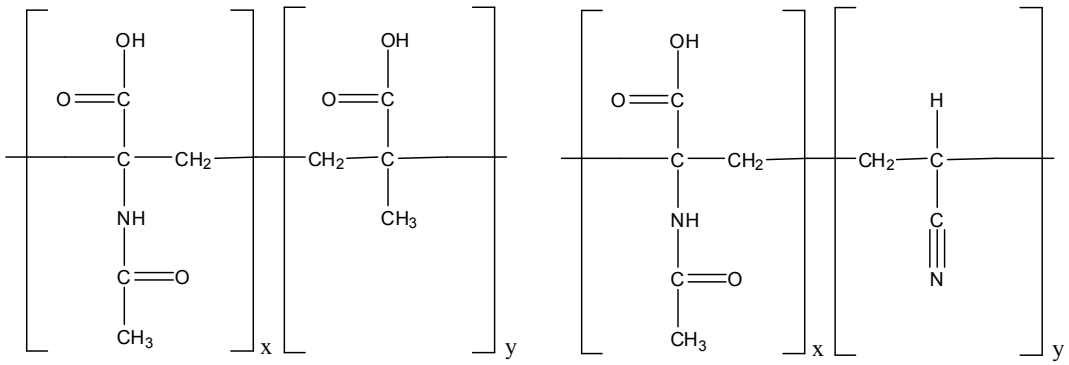

Poly(AAA-co-MAA) Poly(AAA-co-AN)

Figure 2.1 Methacrylic acid and acrylonitrile substituted AAA copolymers.

2.1 Experimental Section

2.1.1 Materials

All chemicals were purchased from Aldrich. All chemicals were used without further purification unless specified otherwise. Dimethylformamide (DMF) was distilled over CaH_2. Methacrylic acid (MAA) was purified by vacuum distillation over $CuCl_2$. Both acrylonitrile (AN) and MAA were passed through basic alumina column to remove the inhibitor. To remove impurities, filtered from 200 nm teflon syringe filters and stored at 4°C after deoxygenation. 2,2'-Azobisisobutyronitrile (AIBN) was purified by recrystallization from methanol prior to use.

2.1.2 Monomer Synthesis

2-Acetamidoacrylic acid (AAA) was synthesized by refluxing pyruvic acid (0.43 moles) and acetamide (0.18 moles) in 300 mL toluene for approximately 4 hr under Argon gas. As the reaction proceed, liberated water was collected in a Dean Stark apparatus until the theoretical amount of water was obtained (3.5 ml). After

cooling to room temperature, monomer crystallized in the reaction pot. White crystals were removed by filtration and recrystallized from hot acetone. Yield varies from 60 to 71%. The melting point of the monomer was determined as 198-199 ºC.

^{1}H NMR (DMSO-d_6): δ (ppm from TMS) 2.02 (-$COCH_3$,s, 3H), 5.65 (CH_2=C, s,1 H, trans to acetylamido group), 6.23 (CH_2=C, s,1 H, cis to acetylamido group), 9.10 (-NH-, s, 1H), 13.26 (-COOH, s, 1H), 2.50 (DMSO-d_6), 3.30 (residual water in DMSO-d_6).

2.1.3 Polymer Synthesis

All polymerizations were carried out at 70°C, in a sealed 50-mL round-bottomed flask with a magnetic stirrer. Solutions were degassed at least for 15 minutes with pure argon. AIBN and 4,4'-Azobis-4-cyanovaleric acid (ACVA) were used as initiators. AIBN was used for polymerizations in DMF and ACVA was used in deionized water. 0,1 % mol of initiator was used on the basis of total amount of monomers.

2.1.3.1 Copolymerization of AAA with AN

Copolymerizations of AAA with AN were carried out in DMF. All polymerizations were terminated by precipitation of the resulting polymer into cold tetrahydrofuran (THF) either after 3 or 12 h of reaction. Isolated polymers were dissolved in deionized water, and purified by dialysis (3,000 molecular weight cut-off cellulose dialysis membrane, CelluseSep T1 Regenerated Cellulose Tubular Membrane) in deionized water over 5 days (water was changed every 12 h) and dried through lyophilization. Copolymer composition was determined by elemental analysis.

2.1.3.2 Copolymerization of AAA with MAA

Copolymerizations of AAA with MAA were carried out both in DMF or in deionized water. Polymer synthesis in *aqueous medium* was done as follows: the pH of the reaction mixture was adjusted to 7.5 with sodium hydroxide prior to the addition of ACVA. 40 min and 12 hour polymerizations were carried out and polymers were quenched in liquid nitrogen. Copolymerization reactions of AAA with MAA *in* DMF, were stopped by precipitation of the resulting polymer into cold diethyl ether after 3 and 24 h polymerizations.

Isolated polymers were dissolved in deionized water, and purified by dialysis (3,000 molecular weight cut-off cellulose dialysis membrane, CelluseSep T1 Regenerated Cellulose Tubular Membrane) in deionized water over 5 days (water was changed every 12 h) and dried through lyophilization. Copolymer composition was determined by elemental analysis.

2.3 Characterization

After dialysis, all copolymers were analyzed by using proton nuclear magnetic resonance (^{1}H NMR) to be sure that polymers are free of impurities such as residual solvent and monomer content. All ^{1}H NMR experiments reported in this study were carried out on a Bruker Ultrashield 300 MHz spectrometer (Gazi University, Ankara, Turkey).

FT-IR spectra of all polymers and monomers were measured with Nicolet FT-IR spectrophotometer from Thermo Scientific Inc. with 2 cm^{-1} resolution. The total carbon, hydrogen and nitrogen contents of the polymers were determined using a Thermo Finnigan Flash EA 1112 CHNS-O Analyzer (İstanbul University, İstanbul, Turkey).

Molecular weight of polymers were measured with a gel permeation chromatography (GPC) (Agilent 1100) equipped with refractive index detector.

Polymer Labs PL Aquagel-OH Mixed 8 µm column was used. Samples were prepared at 2.0 mg/ml concentration and 50 µl injection volumes were used. All of the polymer solutions were filtered through 0.20-µm-pore-size filters before injection. pH 7 buffer containing 0.02% (by weight) NaN_3 at a flow rate of 1.0 ml/min at, 25°C was used for elution. Poly(acrylic acid)-sodium salt standards (Polymer Labs) with narrow polydispersity and with molecular weights ranging from $1.25x10^3$ to $1,10x10^6$ Da was used to construct a calibration curve.

For water insoluble polymers, PSS gram 1000 (pore size 1000 Å; bead size 10 µm; 1000-1000000 Da) column at 35°C was used. A solution of DMF with 0.01% (by weight) LiBr at a flow rate of 1.0 ml/min was used as an eluent. Poly (methyl methacrylate) standards with narrow polydispersity and with molecular weights ranging from 831 to $1,58x10^6$ Da was used to construct a calibration curve.

2.4 Antibacterial Activity Assessment of Polymers

2.4.1 Bacterial Strain

Bacterial cultures of *Bacillus subtilis (B.subtilis)* and *Escherichia coli (E.coli)* were used as gram positive and gram negative microbial test organisms, respectively.

2.4.2 Preparation of LB Broth and LB Agar

LB (Lysogeny Broth) consists of 1% tryptone 0.5% yeast extract and 0.5% sodium chloride. LB broth was dissolved in distilled water to give a concentration of 20 g/L. For LB agar, 15g/L agar was added into 20g/L of LB broth. LB broth and LB agar were sterilized by autoclaving.

The nutrient agar media for bacteria were poured into Petri plates and the solution was allowed to gel or solidify at refrigerator. All the necessary equipments/apparatus for the antibacterial activity testing like culture media, micropipettes tips, glassware etc were sterilized in an autoclave.

2.4.3 Preparation of Inoculum

A representative colony of *Bacillus subtilis (B.subtilis)* and *Escherichia coli (E.coli)* were lifted off with a wire loop and placed in 2 mL of nutrient broth (LB) in a sterile glass test tube. The cultures were incubated in nutrient broth in a rotary shaker at 37°C while being shaken at 220 rpm for overnight. The antibacterial tests were started when the cells reach to mid-log phase, where OD600 nm is between 0.100 and 0.400 (OD value of 1 at 600 nm corresponds to density of 8.8×10^8 cells/mL).

2.4.4 Determination of Antibacterial Activity

Antibacterial activity of the polymers against *B.subtilis* and *E.coli* was evaluated by using the optical density method described as follows: into each sterile test tube containing either *B.subtilis* or *E.coli* bacteria suspension at 6×10^7 cells/mL density, polymer with known concentrations were added. The optical density (OD) values of control (nutrient broth), control bacteria suspension and polymer solutions with bacteria were measured by a spectrometer at 600 nm at different time intervals. The growth of bacteria is measured from the turbidity of the suspension due to light scattering, and can be followed by the rise of optical density. As bacteria multiply in a liquid medium, the medium becomes turbid, or cloudy with cells. The optical density values of control bacteria suspensions were compared with polymer solutions with bacteria.

Polymer samples treated with bacteria were spread on nutrient agar plates after incubation at 37°C for 24 hours to quantify the viable cells (Figure 2.2). The LB agar plates were subsequently cultures in the 37°C for 24 hours and the number of the colonies was counted and photographed.

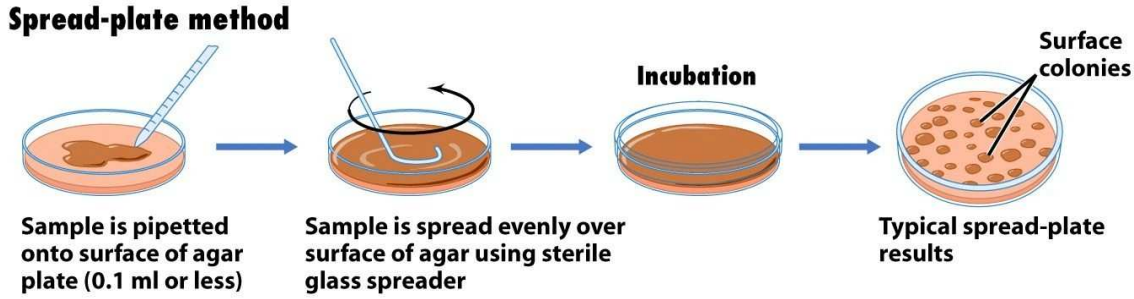

Figure 2.2 Counting bacteria by spread plate method (http://people.rit.edu).

2.5 Results and Discussion

2.5.1 Monomer Synthesis and Characterization

2-Acetamidoacrylic acid (AAA) was synthesized from pyruvic acid and acetamide as shown in Figure 2.3.

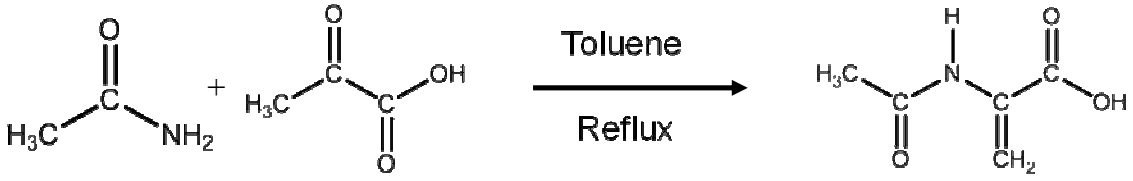

Figure 2.3 Synthesis of 2-Acetamidoacrylic acid.

The monomer structure was confirmed by ATR spectrometer and ^{1}H NMR. Figure 2.4 shows the stacked FTIR spectra of commercial 2-Acetamidoacrylic acid purchased from Aldrich and synthesized 2-Acetamidoacrylic acid (AAA) from pyruvic acid and acetamide. Characteristic carboxylic acid carbonyl stretching appears in the region 1710 cm^{-1} while the carbonyl of amide appears in the region 1634cm^{-1}. The O-H peak produces sharp signal around 3336 cm^{-1}.The bands at 903 cm^{-1} and 1036 cm^{-1} are attributed to =C-H bending. The melting point of the monomer was determined as 198-199 ºC by using Differential scanning calorimetry (DSC) which is

the reported value for the pure substance. 2-Acetamidoacrylic acid is readily soluble in aqueous base, insoluble in water and in inorganic solvents except DMSO and DMF.

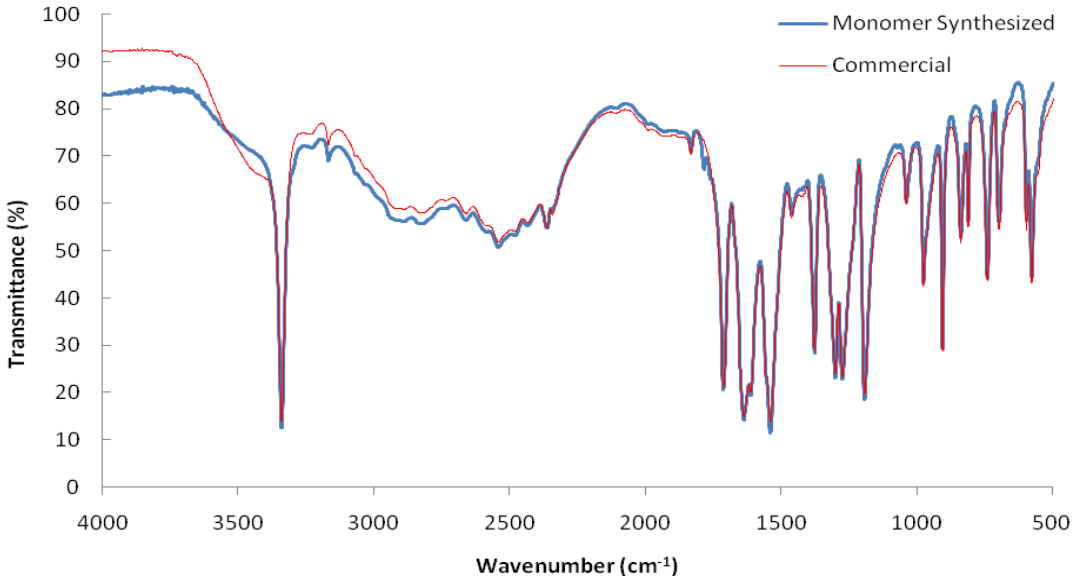

Figure 2.4 FT-IR spectra of commercial and synthesized 2-Acetamidoacrylic acid.

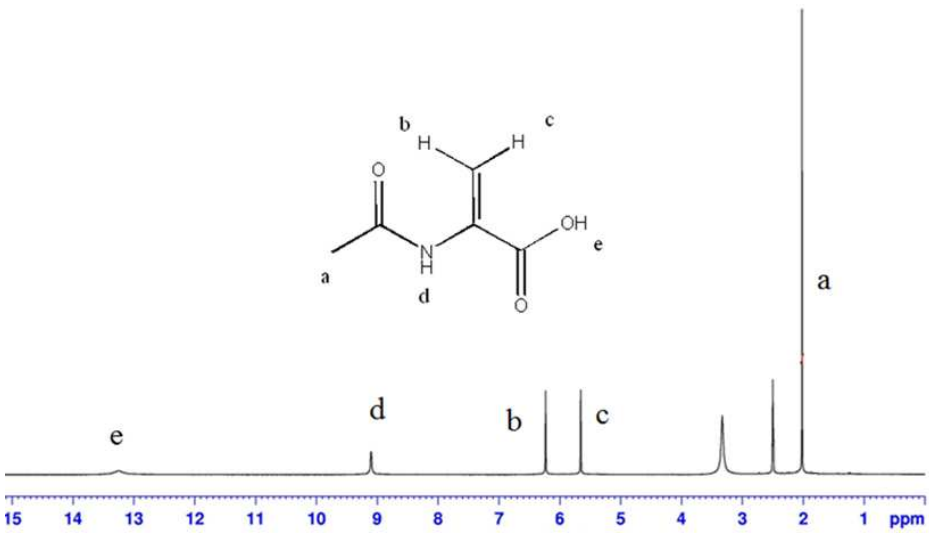

Figure 2.5 ^{1}H NMR (in DMSO-d_6)of 2-Acetamidoacrylic acid.

^{1}H NMR also indicates a pure sample with clear methyl protons at 2.02 ppm vinyl protons 5.65-6.23 ppm and amide and acid protons at 9.10 and 13.26 ppm (Figure 2.5). The peak at 3.30 ppm is coming from residual water in DMSO-d_6.

2.5.2 2-Acetamidoacrylic acid-Acrylonitrile Copolymers

Copolymerization formulations of AN-AAA and polymerization results are given in Table 2.1 and 2.2 for 12h and 3h reactions. Eight different copolymers were formulated. All copolymers had significantly higher content of AAA than feed formulations, indicating higher reactivity ratio of AAA. Polymer conversions are between 30-70 % which is usually too high to calculate reactivity ratios. Therefore, 3h polymerizations were also carried out, resulting in 25-35% conversion which is relatively high. PDI (polydispersity index) of polymers are around 2 and number-average molecular masses (M_n) are within the 25000-130000 g/mol. Moreover, PDI values of polymers obtained from 12h reactions are greater than the PDI values of polymers obtained from 3h reaction. Due to the very short lifetime of active radical species, it is well known that free-radical polymerizations do not allow controlling molecular weight or polydispersity index. In free radical polymerization, the overall kinetics is described by Eq. (1), where the rate of polymerization depends on the monomer concentration [M], initiator concentration [I], initiator efficiency (f) and the rate constants of radical decomposition (k_d), propagation (k_p) and termination (k_t) according to

$$R_p = k_p[M]\,(fk_d[I]/k_t)^{1/2} \quad (1)$$

The kinetic chain length of a polymer, v, is defined as the average number of monomer molecules consumed or polymerized per each free radical that initiates a polymer chain. The kinetic chain length is expressed by Eq. (2)

$$v = k_p\,[M]\,(fk_d[I]/k_t)^{-1/2} \quad (2)$$

The efficiency factor of initiator plays important role in synthesis of the radical species. Ideally, a thermal free radical initiator should decompose readily at the polymerization temperature at the appropriate solvent. However, due to wastage

reactions of radicals such as side reactions or inefficient synthesis of radicals like cage effect of solvent molecules, chain initiation is not always 100% which means that the effective radical concentration is generally less than 100%. In addition, half-life ($t_{1/2}$) of the initiator, the time required to decrease the original initiator amount at a given temperature and solvent by 50%, is the most important criteria for the selection of initiator in polymerization. Both R_p and v depend on the square root of the initiator efficiency, although the rate of free radical polymerization increases as the initiator efficiency increases (because of the generation of greater number of radicals), the kinetic chain length decreases because of the greater termination rate at the higher concentration of radicals. However, it is crucial to notice that, as the rate of free radical polymerization increases with the increasing initiator efficiency (because of the generation of greater number of radicals), the kinetic chain length decreases because of the greater termination rate at the higher concentration of radicals. Therefore, PDI values are obtained from 12 h polymerization reactions are somewhat greater than the PDI values of polymers obtained from 3h reaction. Because of the same reason, the molecular weights of the polymers obtained from 12h reactions are smaller than the molecular weights of the polymers obtained from 3h reaction.

Table 2.1 Molecular characteristics of Poly(AAA-co-AN) prepared in DMF at 70°C for *12 h.*

Polymer Code	Mol % AAA Feed	Mol % AAA in Composition[a]	Rxn Time (hr)	Conversion (%)[b]	M_n [c]	M_w [c]	PDI
PA1	100	100	12	4,58	5106	24907	4,9
PA2	80	93,21		58,29	55496	118150	2,1
PA3	60	94,52		72,79	63599	128570	2,0
PA4	40	79,48		63,66	37222	84116	2,3
PA5	20	58,04		56,52	47812	106720	2,2
PA6	0	0		36,31	25008	53652	2,1

[a] Determined by elemental analysis. [b] Determined gravimetrically. [c] Determined by GPC analysis.

Table 2.2 Molecular characteristics of Poly(AAA-co-AN) prepared in DMF at 70°C for *3 h*.

Polymer Code	Mol % AAA Feed	Mol % AAA Composition[a]	Rxn Time (hr)	Conversion (%)[b]	M_n[c]	M_w[c]	PDI
PA7	100	100	3	7,96	33779	97179	2,9
PA8	80	94,96		30,70	84249	158270	1,9
PA9	60	-		25,60	130670	228090	1,7
PA10	40	73,11		48,88	93749	171930	1,8
PA11	20	70,50		35,54	57122	124450	2,2
PA12	0	0		11,71	28035	56416	2,0

[a] Determined by elemental analysis. [b] Determined gravimetrically. [c] Determined by GPC analysis.

FT-IR results indicate existance of both monomers in the copolymer. Figure 2.6 shows the stacked spectra of acrylonitrile and polyacrylonitrile (PAN) obtained from 12h reaction. Peak at 2229 cm^{-1} is characteristic for nitrile (cyano or C≡N). Due to the presence of residual DMF in the polyacrylonitrile, the infrared spectrum of PA6 gives rise to carbonyl stretching frequency at 1734 cm^{-1}. The band at 2969 cm^{-1} is due to the stretching vibration of CH_2. The bands at 963 cm^{-1} is attributed to =C-H bending mode in acrylonitrile which disappears after polymerization.

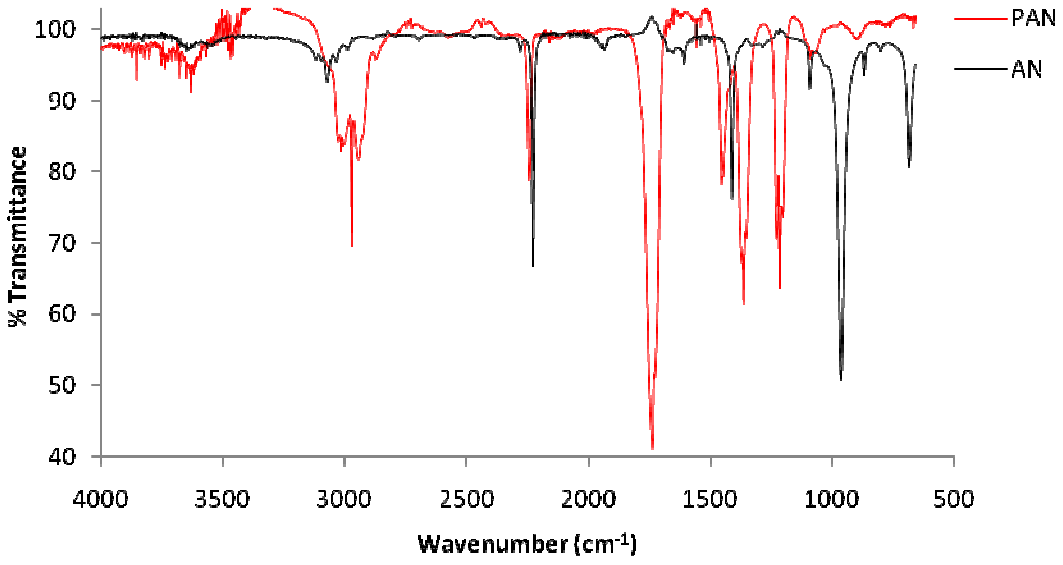

Figure 2.6 FT-IR spectra of acrylonitrile and PA6.

Figure 2.7 shows the stacked FT-IR spectra of all polymers of (AN-AAA) obtained from 12h reaction in DMF. The major functional group that differentiates the acrylonitrile monomer from AAA is the nitrile group. The intensity of the nitrile peak at 2229 cm^{-1} decrease as polymers gets richer in AAA. In literature, some investigators had utilized FT-IR spectrum for the determination of the composition of copolymers of acrylonitrile.[22,23] Firstly, the composition of copolymers were calculated from 2229 cm^{-1} C≡N peak of AN, and 1634 cm^{-1} amide carbonyl peak of AAA. Areas under these bands were calculated to estimate the copolymer ratios. However, the FT-IR spectra were found to be non-suitable for quantification of the composition of copolymers since all of the copolymers were found to have more than 90 mol% AAA in composition. We have tested the method by mixing the monomers in known ratio and calculating the ratio of monomers through FT-IR as described above, but no satisfactory results were obtained. UV-Vis and ^1H NMR of copolymers were also exploited to determine copolymer compositions but all suffer from different problems and produce different answers. In the ^1H NMR of the copolymers, peaks of PAN are superimposed with the peaks of (CH_3 and CH_2) the P(AAA). Thus, no copolymer composition calculation is possible (Appendix1). Therefore, compositions of copolymers were determined by elemental analysis (based on nitrogen content).

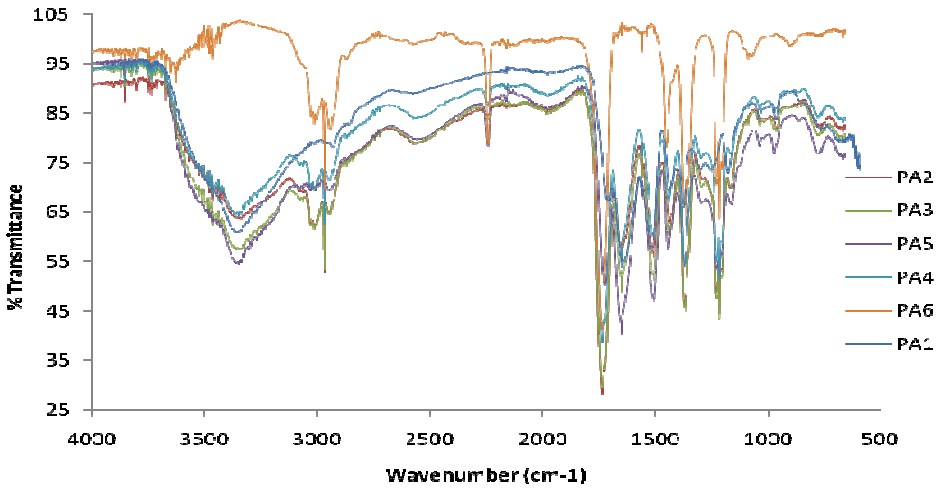

Figure 2.7 FT-IR spectra of copolymers of (AN-AAA) obtained from 12h reaction.

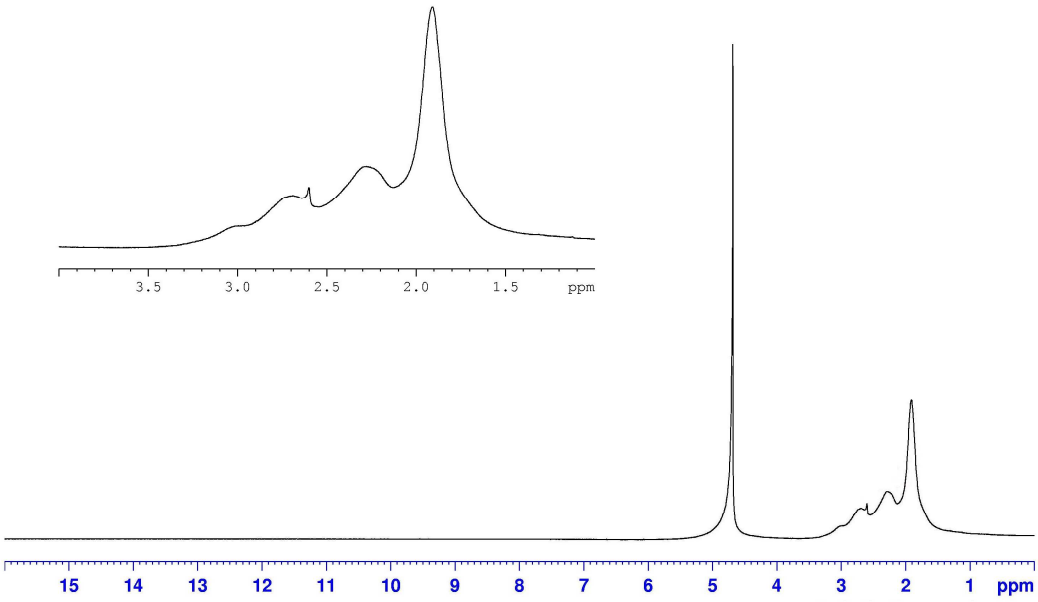

Figure 2.8 ^{1}H NMR (in D_2O)of copolymer of AAA with AN (PA10).

PAN is not water soluble. AAA is not water soluble but its polymer is. All polymers are soluble in water indicating significant incorporation of AAA. Only copolymers containing 80 mol% AN in the feed shows lower solubility in water which means even at such high AN content in feed, significant amount of AAA is incorporated to the polymer backbone. AAA rich copolymers indicates that there should be a significant difference between the reactivity ratios of acrylonitrile and 2-acetamidoacrylic acid. 2-Acetamidoacrylic acid is an acetylamido derivative of acrylic acid. As can be seen in Figure 2.9 at both reaction times AAA was incorporated at much larger extent and all copolymers have more than 50% AAA in the final composition. Conversion is an important factor in determining copolymer composition when there is reactivity difference between the monomers. None of these polymerization sets are suitable for calculating the reactivity ratio between these two monomers experimentally. Usually conversions are kept below 10% to guarantee that radical ends can theoretically find similar amounts of both monomers and the composition is mostly depended on the reactivity not on the relative amounts of the

available monomers. AAA/AN 20/80 ratio in feed produced a copolymer with 58% AAA at 56% conversion and 70% AAA at 35% conversion (Table 2.1 and Table 2.2). This increase in AN incorporation at higher conversions is probably originating from the fact that the more reactive monomer is consumed faster and therefore at extended times there are statistically more opportunity to find the less reactive monomer. The difference decreased as the AAA amount increased in the feed. These results also indicate the unsuitable nature of these copolymers for an accurate experimental reactivity ratio calculation.

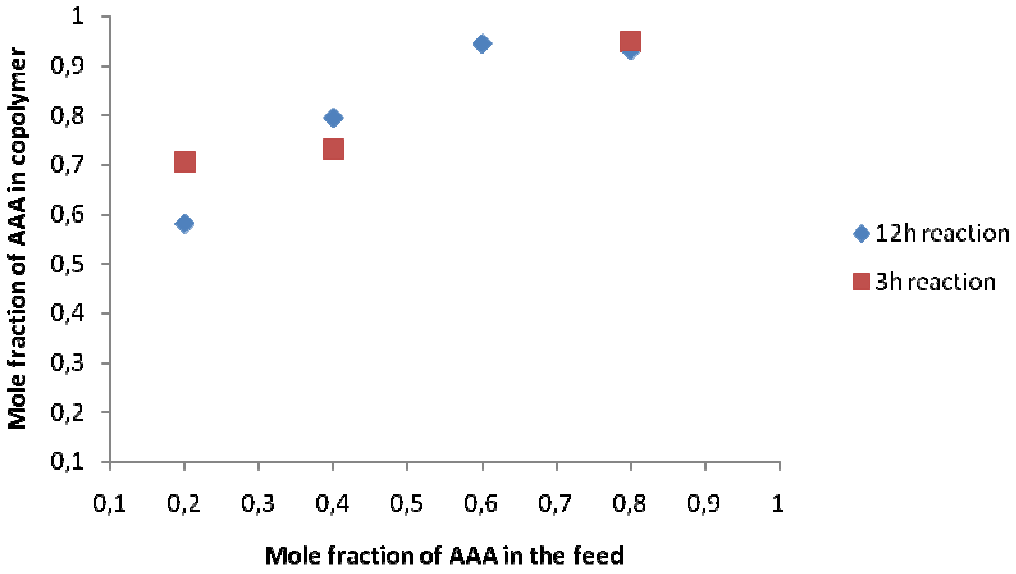

Figure 2.9 Composition curve for the copolymerization of AAA with AN in DMF.

Anyway, from 3 h polymerization reactions the monomer reactivity ratios were tried to be calculated by Tidwell-Mortimer method which ends with a negative reactivity ratio for acrylonitrile. However, a negative reactivity ratio has no physical meaning which indicates an inappropriate model. Yet, from 12 h polymerization reactions by using the same method the monomer reactivity ratios for acrylonitrile (AN) and 2-acetamidoacrylic acid (AAA) were found to be r_{AAA}=7.4048 and r_{AN}=0.2698. Bajaj et al. studied the copolymerization of acrylonitrile with acrylic acid

monomer in DMF at 70°C, using AIBN as initiator.[21] Reactivity ratios were calculated using Kelen-Tüdos method as 0.495 and 2.502, respectively for acrylonitrile and acrylic acid.[21] This result is in agreement with our findings. Larger difference between AAA and AN compared to AA and AN may originate from capto-dative stabilization. Reactivity ratios should be used cautiously but still results indicate that AAA has greater reactivity ratio than acrylonitrile hence, the probability of AN entering the copolymer chain is less as compared to AAA. Therefore, the copolymer obtained will be richer in AAA.

2.5.3 2-Acetamidoacrylic acid-Methacrylic Acid Copolymers

A large reactivity difference between AAA and Styrene was reported.[14] We have found a large reactivity difference between AAA and AN. Part of the reason was postulated as H-bonding and polar interactions between the AAA monomers. H-bonding between the two monomers may decrease the reactivity ratio difference. Formulations for AAA-MAA copolymers and polymerization results are given in Table 2.3 and 2.4 for 24h and 3h reactions in DMF. Polymer conversions for 24h reactions are between 20-50 % which is too high to calculate reactivity ratios. Therefore, 3h polymerizations were also carried out with 8-16% conversion. At low conversions, the propagating radical will preferentially select the monomer based on reactivity. However, at higher conversions, after the consumption of the preferred monomer in the medium the growing polymer radical will add compulsory to the other monomer which is available in the system in excess.

Figure 2.11 and 2.12 show the stacked FT-IR spectra of all polymers of AAA-MAA. The major functional group that differentiates the AAA from methacrylic acid monomer is the amide group of AAA which has a characteristic amide carbonyl stretch at 1600 cm^{-1}. The intensity of the amide peak is greater for the polymers that are richer in AAA. However, asymmetric stretching mode of carboxylate at 1540 cm^{-1} is significant in PA29 and PA28, the polymers that are richer in methacrylic acid. ^{1}H

NMR of the P(AAA-co-MAA) shows separate methyl peaks for MAA and AAA (Appendix 1). However, integration of the peaks yields different ratios from the ratios obtained by the elemental analysis. Because of the poor baseline calibration elemental analysis results were used.

Table 2.3 Molecular characteristics of Poly(AAA-co-MAA) prepared in DMF at 70°C for *24h.*

Polymer Code	Mol % AAA Feed	Mol % AAA Composition[a]	Rxn Time (hr)	Conversion (%)[b]	M_n[c]	M_w[c]	PDI
PA13	100	100	24	33,21	659	669	1,0
PA14	80	-		27,65	27119	76571	2,8
PA15	60	83,80		20,63	11333	31318	2,8
PA16	40	60,73		34,69	30985	80737	2,6
PA17	20	42,11		31,48	26401	62686	2,4
PA18	0	0		45,43	107640	175770	1,6

[a] Determined by elemental analysis. [b] Determined gravimetrically. [c] Determined by GPC analysis.

Table 2.4 Molecular characteristics of Poly(AAA-co-MAA) prepared in DMF at 70°C for *3h.*

Polymer Code	Mol % AAA Feed	Mol % AAA Composition[a]	Rxn Time (hr)	Conversion (%)[b]	M_n[c]	M_w[c]	PDI
PA7	100	100	3	7,96	33779	97179	2,9
PA19	80	73,66		15,91	76510	139860	1,8
PA20	60	60,42		14,79	47299	82879	1,8
PA21	40	57,53		11,11	23297	75118	3,2
PA22	20	39,87		8,54	24043	54888	2,3
PA23	0	0		14,62	68166	144050	2,1

[a] Determined by elemental analysis. [b] Determined gravimetrically. [c] Determined by GPC analysis.

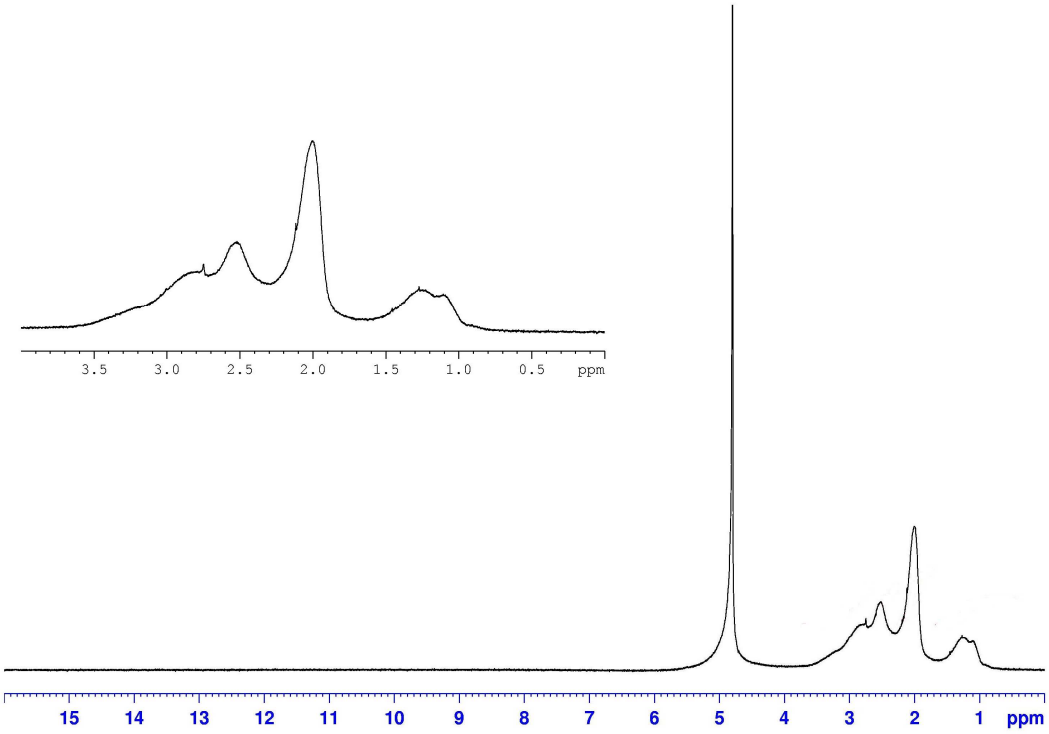

Figure 2.10 ^{1}H NMR (in D_2O) of copolymer of AAA with MAA (PA16).

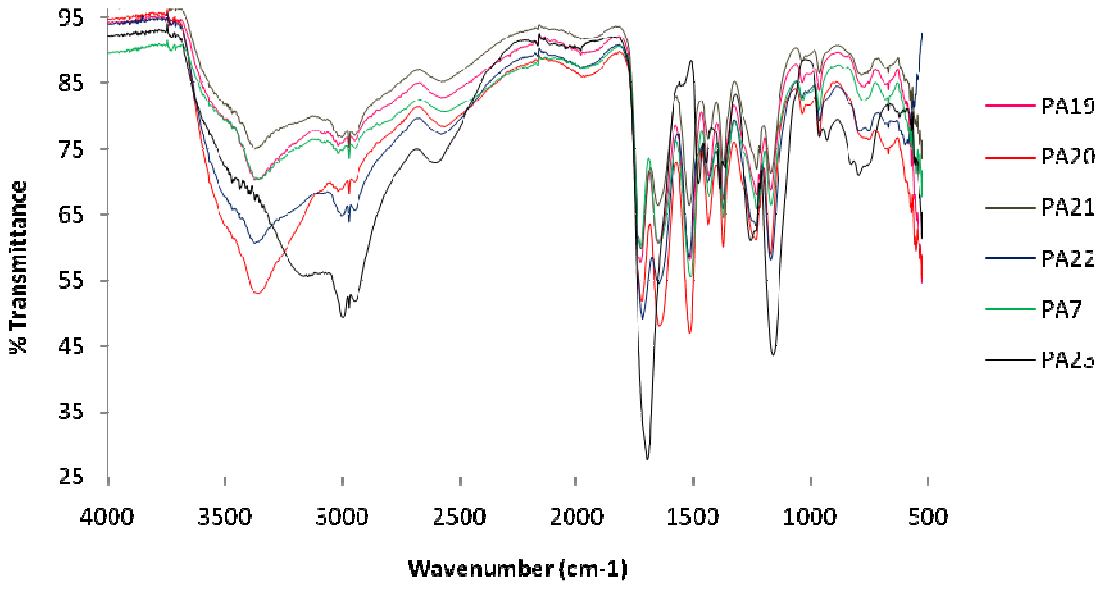

Figure 2.11 FT-IR spectra of copolymers of (MAA-AAA) obtained from 3h reaction.

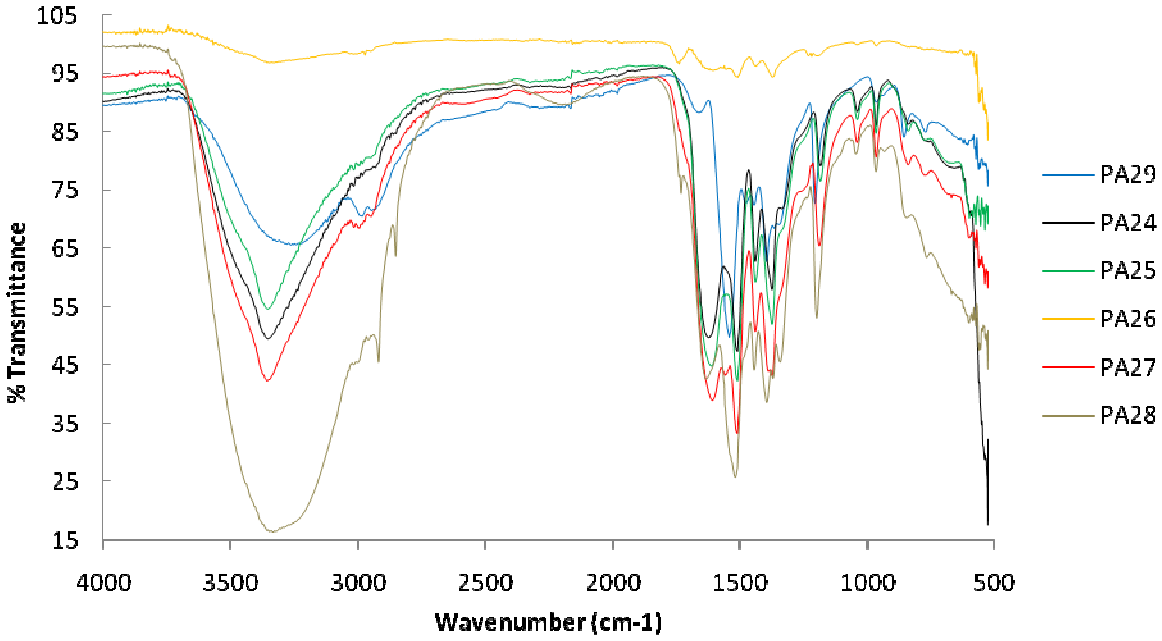

Figure 2.12 FT-IR spectra of copolymers of (MAA-AAA) obtained from 12h reaction in aqueous medium.

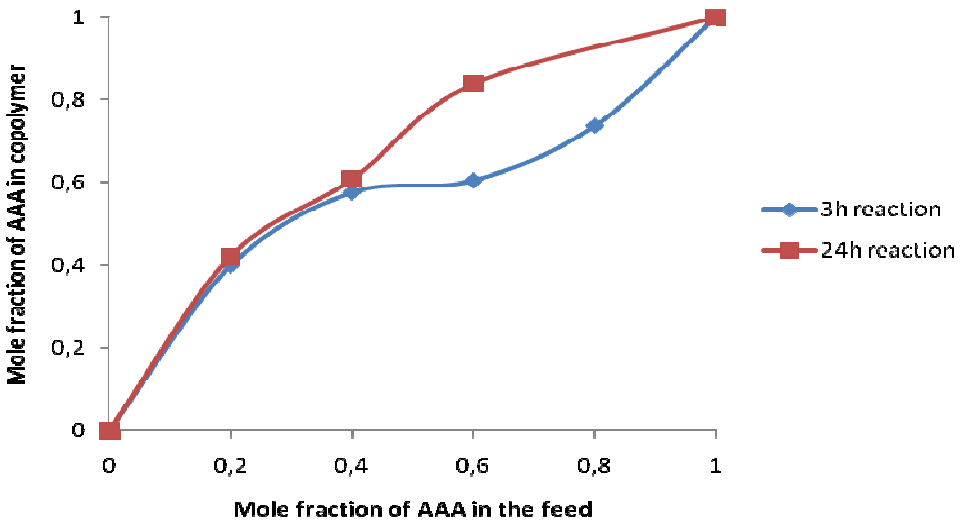

Figure 2.13 Composition curve for the copolymerization of AAA with MAA in DMF.

In the copolymerization reactions carried out in DMF, all copolymers were richer in AAA. Conversions were kept below 16% in 3h reactions. The major

difference between the feed and copolymer composition shows up in 20 and 40% AAA in feed. At and above 60% AAA in feed the copolymer composition is similar to the feed (Figure 2.13). Reactivity ratio of AAA is higher than MAA and at feed compositions where there is plenty of AAA, the preferential consumption of AAA does not change the remaining monomer composition in the pot as much as the cases where AAA is the minor component at low conversions. The monomer reactivity ratios were calculated as r_{MAA}=0.1398 and r_{AAA}=0.5099 with the Tidwell-Mortimer method. AAA is found to have larger monomer reactivity ratio than methacrylic acid. The inverse of the monomer reactivity ratio (1/r) gives the reactivity of a monomer. From these reactivity ratios, the monomer reactivies were calculated as 7.2 and 2.0, respectively for MAA and AAA meaning that AAA is found to be less reactive monomer. This is reasonable because AAA is a captodative monomer and resonance stabilization due to captodative effect stabilizes the propagating radical so that radical reactivity will be less. *Q* and *e* values of 2-acetadimoacrylic acid were calculated to be 2.89 and -0.5, respectively on the basis of monomer reactivity ratios, where $Q = 0.98$ and $e = 0.62$ were used for methacrylic acid. The parameter *Q* describes the resonance factor present in the monomer and the parameter *e* describes the polar factor. The significantly greater *Q* value of 2-acetamidoacrylic acid suggests extensively resonance stabilized AAA radicals. In addition, negative values of e indicate electron rich monomers, while positive values of e indicate electron deficient monomers. Tanaka reported *Q* and e value of 2-acetamidoacrylic acid as 2.43 and 0.89, respectively from the reactivity ratios calculated in AAA-styrene copolymerization in DMSO. [14]

MAA can do hydrogen-bonding with both AAA and reaction solvent, DMF. The presence of hydrogen-bonding can promote the rate in the propagation step by increasing the effective local monomer concentrations at the radical sites (sometimes referred to as “Bootstrap” effect) which would influence the reactivity ratios. The effective free-monomer and/or radical concentration differ from the bulk at the site of the growing chain when there is a monomer partitioning due to the preferential

presence of the co/monomers around the growing polymer chain or if one of the monomers is a poor solvent for the resulting polymer.[24]

As noted above, concerning carboxylic acid monomers such as methacrylic and 2-acetamidoacrylic acid, the hydrogen-bonding should have an influence on the rate of polymerization and copolymer composition. Interestingly, monomer conversion in AN-AAA pair is much higher than MAA-AAA pair under identical conditions (Table 2.2 and 2.4). Although acrylonitrile is not capable of doing intramolecular hydrogen-bonding it has large dipole moment of 3.9 D because of the nitrile group which leads to strong intrachain and interchain interactions (Figure 2.14). The dipole moment of methacrylic acid is 1.65 D which is smaller than the dipole moment of the acrylonitrile. Considering this, there can be dipole-dipole and H-bonding interactions between 2-acetamidoacrylic acid and acrylonitrile (between the nitrogen atom of nitrile unit of acrylonitrile and hydrogen atom of the acetamido group of 2-acetamidoacrylic acid) which can increase the reactivity of the monomer and/or radical in the propagation step by a polar effect.

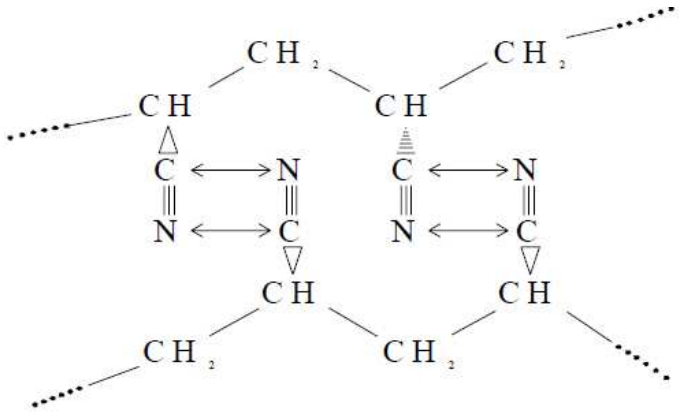

Figure 2.14 The dipole-dipole bonds present in the poly(acrylonitrile) due to the polarity of the nitrile group.

Conversion of AN-AAA in 3 h are around 45-49% but MAA-AAA reaches these values in 24 h (20-35%). When PA10 and PA19 are compared, about 73% AAA in the copolymer is obtained in 3h with 40% AAA in feed for AAA-AN, but with 80%

AAA in AAA-MAA. Besides for PA10 conversion is 49% and for PA19 16%. So, rate of reaction for MAA-AAA reaction is lower but the difference in reactivity ratio is more dramatic in case of AN and AAA. Hydrogen bonding is usually a stronger interaction than dipole-dipole. However, AAA and MAA can do hydrogen bonding with the solvent as well. But, beyond this, AN radical is more reactive than MAA or AAA radical since it is a secondary radical.

Hydrogen bonding is an important factor which can exaggerate the value of a reactivity ratio for acidic monomers by increasing the local concentration of monomer in the vicinity of propagating radicals. The polymerization of methacrylic acid and AAA is known to be sensitive to pH of the solution.[25] The copolymerization of methacrylic acid and 2-acetamidoacrylic acid was carried out in *aqueous medium* at pH of 7.5 in order to eliminate the effect of hydrogen bonding on the reactivity ratio. pH of 7.5 was chosen because at this pH all –COOH will be ionized. Thus, the participation of a monomer unit to the propagating radical will not be more likely due to the electrostatic repulsion between monomer radicals and macro radicals. Copolymerization formulations of MAA-AAA and polymerization results are given in Table 2.5 and 2.6 for 12h and 40 min. reactions in *aqueous medium* at pH 7.5. Monomer conversions in 12h are between 5-100 % which is too high to calculate reactivity ratios. However, 40 min. reactions gave 0.09-3.72% conversions.

Table 2.5 Molecular characteristics of Poly(AAA-co-MAA) prepared in aqueous medium at 70°C for *12h.*

Polymer Code	Mol % AAA Feed	Mol % AAA Composition[a]	Rxn Time (hr)	Conversion (%)[b]	M_n[c]	M_w[c]	PDI
PA24	100	100	12 hr	61,39	237650	301050	1,3
PA25	80	69,43		50,38	302220	355100	1,2
PA26	60	58,15		64,21	117550	215750	1,8
PA27	40	41,75		59,14	26204	52119	2,0
PA28	20	23,17		4,6	69229	123870	1,8
PA29	0	0		100	200560	268420	1,3

[a] Determined by elemental analysis. [b] Determined gravimetrically. [c] Determined by GPC analysis.

Table 2.6 Molecular characteristics of Poly(AAA-co-MAA) prepared in aqueous medium at 70°C for *40minutes*.

Polymer Code	Mol % AAA Feed	Mol % AAA Composition[a]	Rxn Time (hr)	Conversion (%)[b]	M_n[c]	M_w[c]	PDI
PA30	100	100	40 min	0,09	3107	5830	1,9
PA31	80	70,18		0,56	4569	9258	2,0
PA32	60	66,68		1,69	10755	34099	3,2
PA33	40	61,10		1,45	18328	67109	3,7
PA34	20	58,97		3,37	40511	111520	2,8
PA35	0	0		3,72	63144	131530	2,1

[a] Determined by elemental analysis. [b] Determined gravimetrically. [c] Determined by GPC analysis.

Polymerization of 12 h provided copolymer compositions similar to feed composition since conversions were quite high (50-60%) except one. On the other hand, 40 min. reactions provided mostly AAA rich copolymers at very low conversions. The reactivity ratio of the AAA should be significantly greater than methacrylic acids's according to these findings. However, major impact of the reactivity ratio difference showed itself again for feed composition with less than 60% AAA just like the case in DMF.

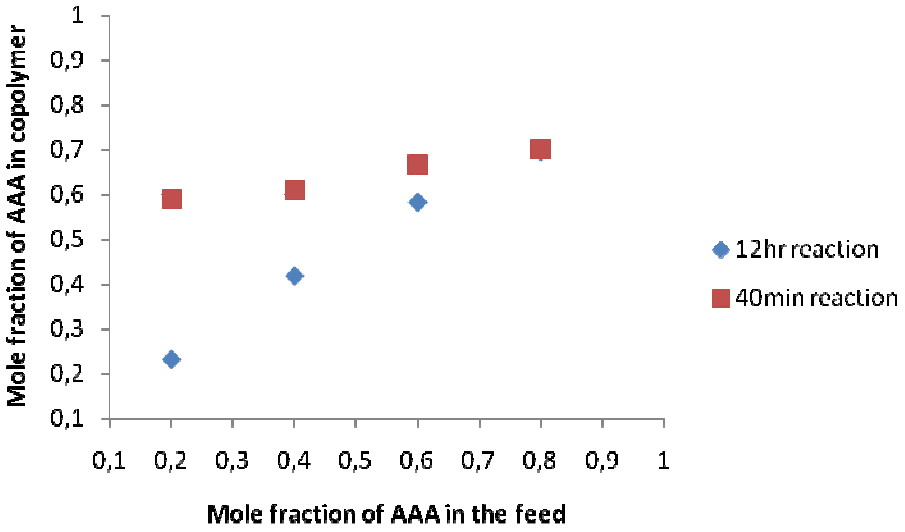

Figure 2.15 Composition curve for the copolymerization of AAA with MAA in H_2O.

Anyway, from 40 min. polymerization reactions the monomer reactivity ratios were tried to be calculated by Tidwell-Mortimer methods which ends with a negative reactivity ratio for methacrylic acid, similar to results obtained from polymerizations done in DMF in 3h. Although monomer conversions are below 10%, a negative reactivity ratio has no physical meaning which indicates an inappropriate model. Yet, from 12 h polymerization reactions by using the same method the monomer reactivity ratios for methacrylic acid (MAA) and 2-acetamidoacrylic acid (AAA) were found to be r_{AAA}=0.4808 and r_{MAA}=0.5960. DMF polymerizations in 24h provided a more dramatic difference between the two monomers: r_{MAA}=0.1398 and r_{AAA}=0.5099. However, these results are not reliable since conversions are very high. From 12 h polymerization data, the greater reactivity ratio of methacylic acid is understandable because more methacrylic acid monomers will be incorporated into the copolymer at higher conversions. However, due to the presence of captodative stabilization it is expected that the reactivity ratio of AAA will be significantly greater than the reactivity ratio of methacrylic acid. Even though the absence of reliable reactivity ratio values, significant incorporation of AAA at lower conversions indicates that the greater reactivity ratio of AAA compared to methacrylic acid which also means that elimination of hydrogen bonding has no influence on the monomer reactivity ratio. In here, the most important issue to be considered is the resonance factor of AAA.

In the case of copolymers of MAA-AAA prepared in DMF from 24h reaction, it can be seen that molecular weights and conversions are significantly lower than that of copolymers prepared in aqueous medium in 12h. In addition to that, PDI are narrower for polymers synthesized in the aqueous medium (Table 2.3 and 2.5). This should be due to the chain transfer effect of the solvent, which is quite important for free radical polymerizations. While the chain transfer constant of water is almost zero, the chain transfer constant of DMF is 2.8×10^4 at 50°C.[24] The possibility of chain transfer to monomer and initiator should not be ignored. Generally, chain transfer to monomer is low because the reaction involves the hemolytic cleavage of a strong vinyl C-H bond (Figure 2.16).[24] However, carbonyl compounds such as acids have

higher chain transfer constants because of the stabilization of the radical by adjacent oxygen or carbonyl group.[24] The major difference between the two polymerizations to consider is the adjustment of pH to 7.5 in aqueous medium. At this pH, all of the methacrylic acid monomers (pK_a= 4.66) are deprotonated so that they are converted to carboxylate anions. Therefore, they can not act as a chain transfer agents. However, chain transfer from methacrylic acid monomers will be significant in DMF since carboxylic acid groups are not deprotonated.

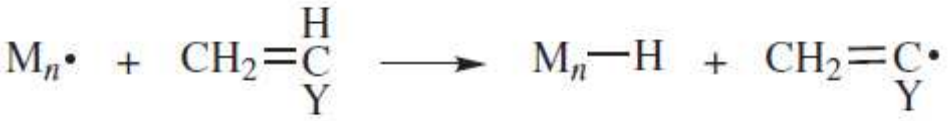

Figure 2.16 Chain transfer to monomer in free radical polymerization.

2.5.4 Turbidity Measurements of Polymers Treated With *E.coli* and *B.subtilis*

Estimating turbidity is an easy and rapid way of monitoring bacterial growth. The turbidity measurement can be done with a spectrophotometer which can measure the amount of light passing through a cell (transmittance). As the bacteria cell population increases in a liquid medium, the medium becomes turbid or cloudy so that less light will be detected by the spectrophotometer. Both low and high conversion polymers were used for antibacterial testing of copolymers. Figure 2.17 and 2.18 shows the growth rate of *E.coli* and *B.subtilis* treated with various polymer samples as measured by the transmittance at 600 nm. The growth of *E.coli* and *B.subtilis* controls (in the absence of polymers) is significantly faster than the *bacteria* treated with polymers (Figure 2.17 and 2.18). The capability of the polymers to inhibit the growth of microorganisms can clearly be seen from the OD (optical density) measurements. However, in order to determine % of death microorganisms viable cell count was done with spread plate method. In the viable cell count, a bacterial colony is counted after 24 hours. It takes some time for colonies to become visible to the naked eye. It is based on the assumption that each viable cell growing on the surface of the agar medium can yield one colony.

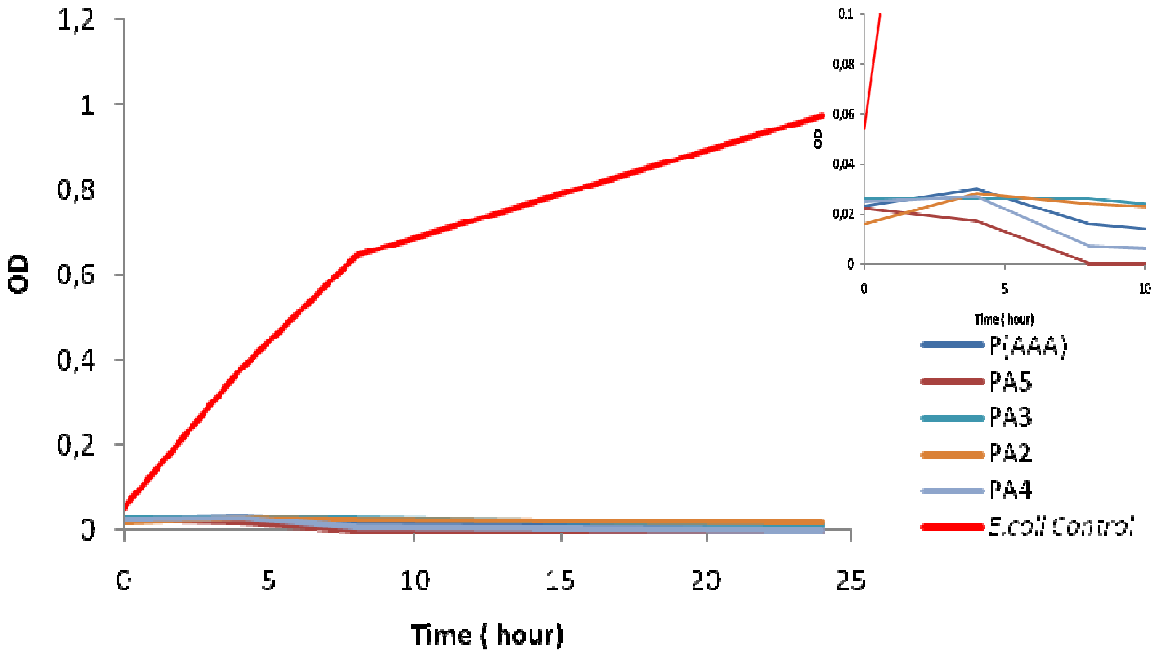

Figure 2.17 Growth inhibition of *E.coli* treated with 12 mg/ml of various polymers.

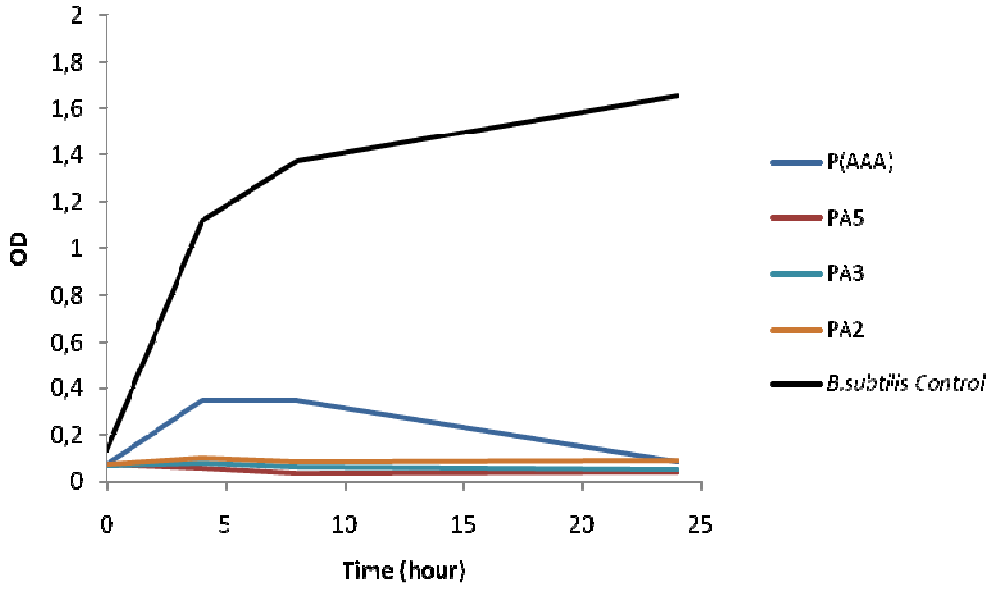

Figure 2.18 Growth inhibition of *B.subtilis* treated with 12 mg/ml of various polymers.

In Figure 2.19, the difference in the turbidity of the solutions can be noticed. While the nutrient medium for the microorganisms is very clear, the medium containing *E.coli* is very turbid and the turbidity of the polymer solution containing bacteria in it is greater than the nutrient medium due to the presence of the bacteria cell population. In the tubes where bacteria were incubated with P(AAA), dead microorganisms due to the antibacterial effect of the polymer can be seen at the bottom of the test tubes. As the bacteria precipitates out of the solution, the turbidity of the solution decreases.

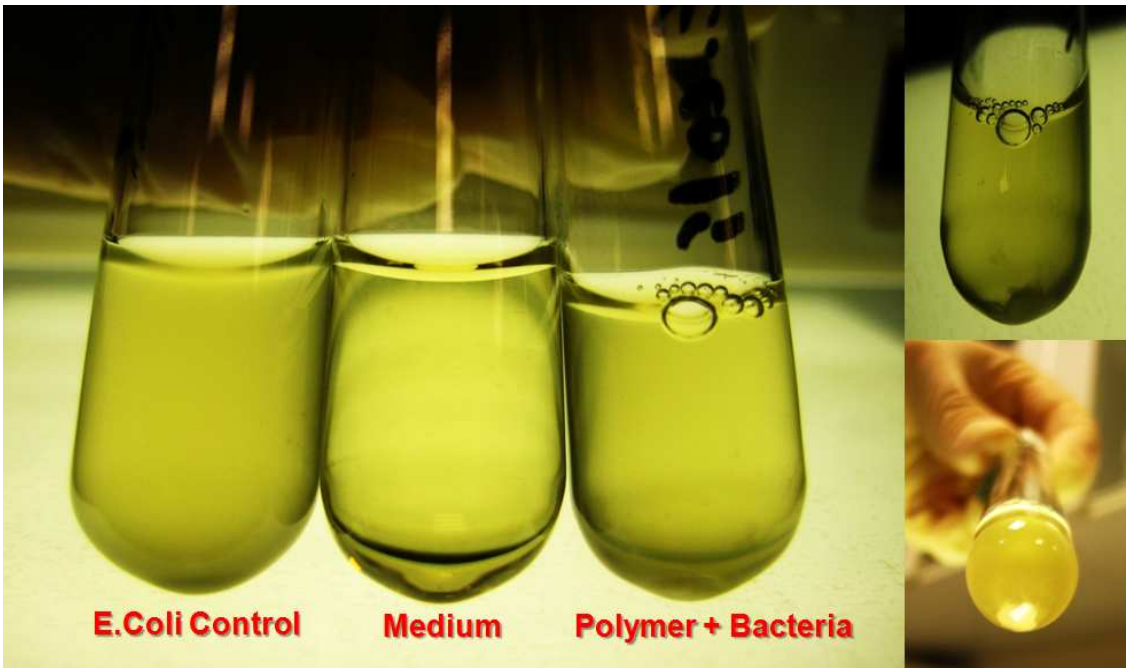

Figure 2.19 Growth inhibition of *E.coli* treated with 8 mg/ml of P(AAA).

In the literature, there are many efforts for obtaining poly (acrylonitrile) fibers with antibacterial properties. The reason for that is; poly (acrylonitrile) is widely used in the manufacture of blankets, carpets and clothing such as sweaters, socks, and sportswear. Therefore, it is very important to bring in antibacterial properties to poly(acrylonitrile) for the well-being of the human healthcare. Acrylonitrile monomer has no effect on the growth of microorganisms which was verified with the colony counting method. We determined that 12 mg/ml of poly (acrylonitrile) can able to kill

88,23% of *E.coli* and 93,18% *B.subtilis* but these numbers are not enough to call poly(acrylonitrile) as a antibacterial polymer. In order to call a material as "antibacterial" it should kill 99,9% (log3 reduction) of the bacteria. At the dose of 12 mg/ml, AAA monomer kills 100% of *E.coli* and *B.subtilis*.

Table 2.7 Percentages of dead bacteria caused by the copolymers of AAA-AN.

Monomers in feed-reaction time	Code	Mol% DHA in Composition	% Dead		% Dead	
			12mg/ml		6mg/ml	
			E.coli	*B.sub*	*E.coli*	*B.sub*
AAA20AC80-12hr rxn	PA5	58,04	99,9259	99,9999	99,9999	-
AAA40AC60-12hr rxn	PA4	79,48	99,9999	99,9999	99,9999	-
AAA60AC40-12hr rxn	PA3	94,52	99,9999	99,9999	99,9999	-
AAA80AC20-12hr rxn	PA2	93,21	100	99,9999	99,9999	-
AAA40AC60-3hr rxn	PA10	73,11	99,9999	-	-	-
AAA20AC80-3hr rxn	PA11	70,50	100	99,9999	99,9999	99,9999

Percentages of dead bacteria caused by the copolymer of AAA-AN are given in Table 2.7. 12 mg/ml of poly (2-acetamidoacrylic acid) can able to kill 100% of bacteria. Test has been conducted with 6 mg/mL for only *E.coli* but same activity was obtained. For the first time in literature, we show that poly (2-acetamidoacrylic acid) is highly antibacterial. All copolymers have at least log3 reduction (99.9% killing) which is enough for many applications. However, all copolymers, except PA5 (against *E.coli*) which contains 58.04% AAA in composition show high antibacterial activity with 99.9999 (log6 reduction) at dose of 12 mg/mL. Copolymers with lower AAA in copolymer composition was not attempted since at 58% we have obtained only 99.9% reduction. At 6 mg/mL probably all copolymers would have same activity based on data obtained with PA11 and *E.coli*. All in all, the copolymers enhance the antibacterial properties of poly (2-acetamidoacrylic acid).

The antibacterial effect of poly (2-acetamidoacrylic acid) against *B.subtilis* can be seen in Figure 2.20. One of the plates is containing only nutrient medium. The absence of a colony indicates that the nutrient medium is free of contaminations and

we had worked under sterile conditions. The medium containing *B.subtilis* has a dilution factor of 10^{10} and the presence of three colonies on the plate meaning that the original inoculum has $3x10^{10}$ colonies. The plate that contains 8 mg/ml of poly (2-acetamidoacrylic acid) polymer has only one colony which means 100% of microorganisms are killed when the dilution factor is taken account.

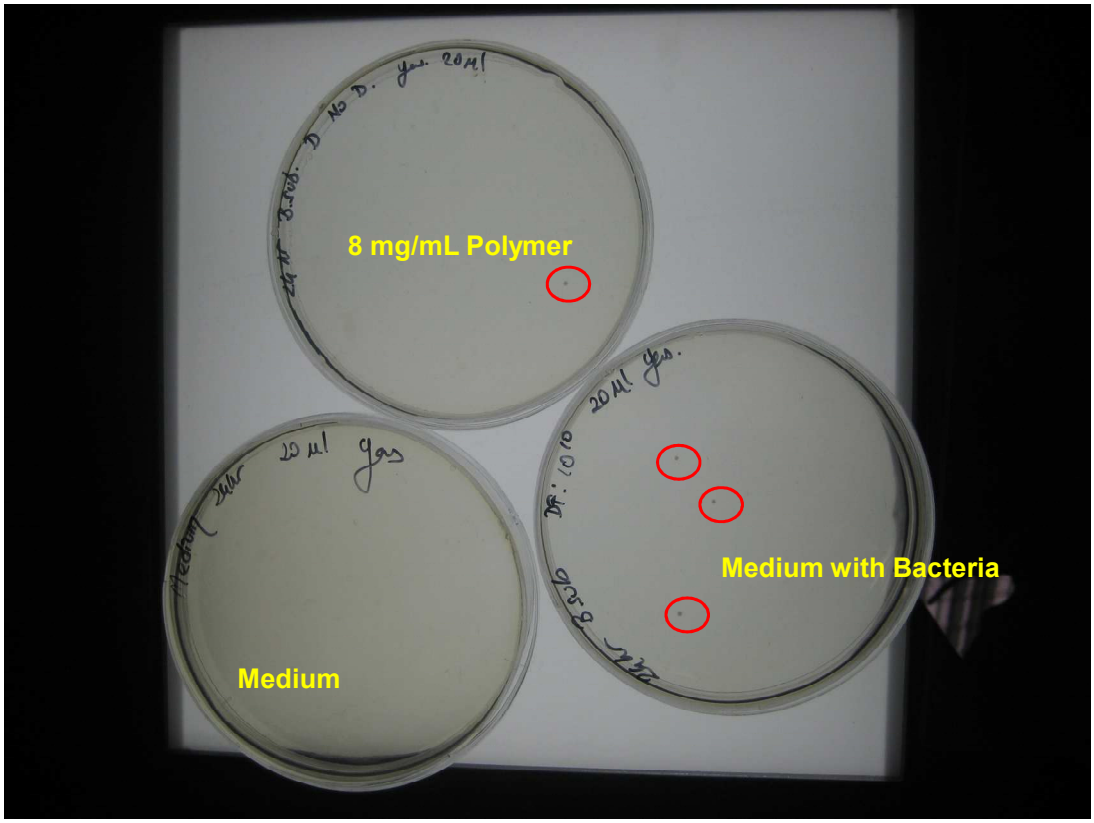

Figure 2.20 Antibacterial effect of poly (2-acetamidoacrylic acid) against *B.subtilis*.

Percentages of dead bacteria caused by the copolymer of AAA-MAA are given in Table 2.8. At dose of 12mg/ml, poly (methacrylic acid) (PA23) can kill 99,98% of *E.coli* and 100% *B.subtilis*. Up to now, it is very interesting that in literature no one has reported the antibacterial property of poly (methacrylic acid). In addition, since the result of antibacterial test of poly (methacrylic acid) belong to different experimental conditions, any contaminations in equipments/apparatus for the antibacterial activity testing like micropipette tips, glassware etc could affect the results. Therefore, results should be evaluated with suspicion. For the copolymers,

incorporation of 39.87% AAA in copolymer is enough to bring excellent antibacterial properties (log6 reduction) poly (methacrylic acid) (against *E.coli*). The best antibacterial activity against microorganisms was achieved by PA16 which contains 60.73% AAA in copolymer composition.

Table 2.8 Percentages of dead bacteria caused by the copolymers of AAA-MAA.

Monomers in feed-reaction time	Code	Mol% DHA in Composition	% Dead	
			12mg/ml	
			E.coli	*B.sub*
DHA20MA80-3hr rxn in DMF	PA22	39,87	99,9999	100
DHA40MA40-24hr rxn in DMF	PA16	60,73	100	99,9999
DHA60MA60-24hr rxn in DMF	PA15	83,80	99,9999	99,9999
Poly(methacrylic acid)- 24hr rxn in DMF	PA18	0	99,9871	100

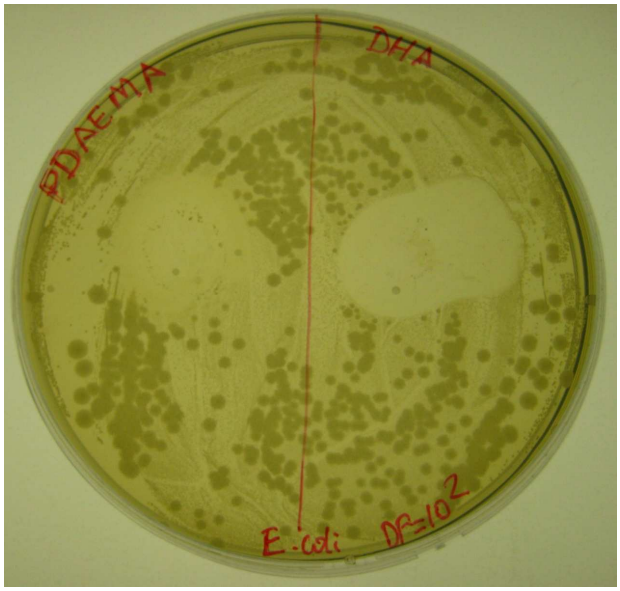

Figure 2.21 Zone of inhibition of poly (2-acetamidoacrylic acid) and PDMEMA against *E.coli*.

Lastly, the antibacterial effect of poly (2-acetamidoacrylic acid) was double checked with the zone of inhibition test. As a reference, we chose poly (2-dimethyl amino ethyl) methacrylate (PDMEMA). 30 mg polymers were pressed as pellets and

placed on the agar plate which contains *E.coli.* After 24h incubation, the zone of inhibition by the polymer samples was photographed (Figure 2.21). At the right hand side, zone of inhibition by poly (2-acetamidoacrylic acid) can be seen clearly. The antibacterial activity of poly (2-acetamidoacrylic acid) seems to be superior to PDMEMA which is known as antibacterial polymer[32]. The bacteria can not reach or survive around poly (2-acetamidoacrylic acid).

2.6 Conclusions

Copolymers of AAA monomer with AN and MAA were successfully synthesized by free radical polymerization. All polymers are soluble in water indicating significant incorporation of AAA both at low and high conversions of (AAA-AN) copolymerizations in DMF. This is mainly because of the significant difference between the reactivity ratios of acrylonitrile and 2-acetamidoacrylic acid. From 12 h polymerization reactions the monomer reactivity ratios for acrylonitrile (AN) and 2-acetamidoacrylic acid (AAA) were found to be r_{AAA}=7.4048 and r_{AN}=0.2698 meaning that the probability of AN entering the copolymer chain is less as compared to AAA. Therefore, the copolymer obtained will be richer in AAA.

In case of MAA-AAA copolymerizations in which the comonomer MAA can also do H-bonding with AAA and itself, AAA incorporated in greater amounts than in feed especially at low conversions. From 3h polymerization reactions in DMF, the monomer reactivity ratios were calculated as 0.1398 and 0.5099 with Tidwell-Mortimer method, respectively for methacrylic acid and 2-acetamidoacrylic acid. From the reciprocal of a reactivity ratio, the reactivity of monomers were calculated as 7.2 and 2.0, respectively for MAA and AAA indicating that AAA is found to be less reactive polymer radical toward methacrylic acid monomer. This is reasonable because the presence of captodative groups on AAA radical gives rise to extra resonance stabilization so decreases the reactivity of the corresponding propagating radical. Monomer reactivity ratio depends on the parameter *Q*, which describes the resonance factor present in the monomer, and the parameter *e*, which describes the

polar factor. *Q* and e value of 2-acetamidoacrylic acid as 2.89 and -0.5, respectively from the reactivity ratios calculated in AAA-MAA copolymerization in DMF where the chosen reference values of $Q = 0.98$ and $e = 0.62$ for methacrylic acid. Yet, the resonance factor is more important than the polar factor, meaning that the value of a monomer reactivity ratio mostly depends on *Q*. Monomers with high *Q* values indicate extensively resonance stabilized radicals. The significantly greater *Q* value of 2-acetamidoacrylic acid compared to methacrylic acid suggests that highly resonance stabilized radical due to captodative effect. Since these two carboxylic acid monomers can do hydrogen bonding which can exaggerate the reactivity ratio values, the copolymerization reaction was carried out in *aqueous medium* at pH of 7.5 to eliminate hydrogen bonding between the two. Even though the absence of reliable reactivity ratio values, incorporation of less methacrylic acid at lower conversions indicates that the smaller reactivity ratio of methacrylic acid compared to 2-acetamidoacrylic acid. Therefore, presence or elimination of hydrogen bonding between the two monomers has no dramatic influence on the monomer reactivity ratio because the most dominant factor that plays critical role is the resonance factor of 2-acetamidoacrylic acid. Moreover, monomers with electron rich double bonds have negative *e* values. The major functional group that differentiates the 2-acetamidoacrylic acid from methacrylic acid monomer is the acetylamido group. The presence of additional carbonyl group in the 2-acetamidoacrylic acid with respect to methacrylic acid explains the determination of negative *e* value. The *Q*-*e* values can be used to make useful predictions about the copolymerization behavior of monomer pairs. For instances, monomers with very different Q values copolymerize poorly since a resonance stabilized radical will be preferred to a less stabilized radical. Although *Q* and e value of 2-acetamidoacrylic acid can not be determined from the copolymerization of acrylonitrile, the significant incorporation of AAA both at low and high conversions of copolymerizations indicates important difference between the reactivity ratios of two monomers which should originate from the very different values of *Q*. Thus, 2-acetamidoacrylic acid does not copolymerize well with acrylonitrile.

Table 2.9 Monomer reactivity ratios in radical copolymerization.

M_1	r_1	M_2	r_2	Solvent
2-Acetamidoacrylic acid	0.53	Sytrene[14]	0.11	DMSO
	0.5099	Methacylic acid	0.1398	3h in DMF
	0.4324	Methacylic acid	0.0652	40 min. in H_2O
	7.4048	Acrylonitrile	0.2698	12h in DMF
Methacrylic acid	3.45	Acrylonitrile[21]	0.265	DMF

For the first time in literature, we show that poly (2-acetamidoacrylic acid) has highly antibacterial activity. We synthesized copolymers of AAA and AN and found that at dose of 12 mg/mL all copolymers (log6 reduction, 99.9999% killing), except PA5 (against *E.coli*) which contains 58.04% AAA (log3 reduction, 99.9% killing) in composition have both good antibacterial activity against *E.coli* and *B.subtilis*. For both microorganisms at dose 6 mg/mL, PA11 which contains 70.50% AAA in composition has log6 reduction. Probably other copolymers would have same antibacterial effect based on data obtained with PA11. Therefore, it is shown that incorporation of AAA in AAA-AN copolymers brings in antibacterial properties.

For the copolymers of AAA and MAA, the presence of 39.87% AAA in copolymer composition is enough to bring excellent antibacterial properties (log6 reduction). The best antibacterial effect against both microorganisms was obtained by PA16 which contains 60.73% AAA in copolymer composition. Many factors control or affect antibacterial properties of polymers. Although the reasons behind the antibacterial effect of poly (2-acetamidoacrylic acid) are not known, have shown that poly (2-acetamidoacrylic acid) is a novel antibacterial polymer and the copolymers enhance the antibacterial properties of poly (2-acetamidoacrylic acid).

Chapter 3

DEVELOPMENT Of POLY(2-ACETAMIDOACRYLIC ACID) STABILIZED QUANTUM DOTS

Research presented in this dissertation addressed the need for improvement of aqueous stability and cytotoxity of quantum dots. Chapter 3 mainly focuses on evaluation of Poly(2-acetamidoacrylic acid) as a coating for luminescent CdS quantum dots and investigation of the effect of binary coating systems on CdS properties. Based on our previous experience combination of small capping molecules with macromolecular stabilizers may bring out a synergy on particle properties. Poly(dehydroalanine)s can be excellent biocompatible coatings for nanoparticles. It is water soluble, potentially biocompatible and open to development of various derivatives. Based on our previous experience combination of small capping molecules with macromolecular stabilizers may bring out a synergy on particle properties. Therefore, the influence of binary coating systems comprised of P(AAA)/cysteine or P(AAA)/ 3-mercaptopropionic acid on CdS properties were also investigated. Cysteine is one of the most popular biocompatible coatings and 3-MPA (3-mercaptopropionic acid) is probably the most widely used coating for QDs. Specifically, ability of P(AAA) and its mixtures with cysteine and 3MPA to coat particle surface, prevent aggregation and oxidation as well as improve optical properties and biocompatibility were investigated.

3.1 Materials

All the chemicals used were of analytical grade or of the highest purity commercially available. Sodium sulfide trihydrate ($Na_2S.3H_2O$), (R)-(+)-Cysteine, cadmium acetate dehydrate ($Cd(CH_3COO_2)\cdot 2H_2O$) ,Rhodamine B were purchased from Merck. Sodium hydroxide and acetic acid were purchased from Aldrich and LaCheMa, respectively. High purity water was used from Milli-Q water (Millipore) system.

3.2 Experimental Section

3.2.1 Synthesis of Aqueous (R)-(+)-Cysteine and Poly(AAA) Capped CdS QDs

30.0 mg of $Cd(CH_3COO_2)\cdot 2H_2O$ was dissolved in 90 mL of deoxygenated water in a three-necked round bottomed flask under continuous stirring and Argon flow. Desired amount of coating material P(AAA) or its mixture with cysteine was added to the cadmium containing solution and the pH was adjusted to 7.5 with dilute NaOH. The sulfide solution was prepared by dissolving 2.8 mg of $Na_2S.3H_2O$ in 10 mL of water and added to deoxygenated Cd-solution at room temperature. Reactions were carried out for 1 hour at 50°C under Argon. All QDs were stored in fridge. Before characterizations, all samples were prepared by multiple washing of QDs with water through Amicon ultrafiltration tubes (Amicon Ultra-15 Regenerated Cellulose 3000 MWCO) at 3800 rpm in order to remove excess organic materials or inorganic ions from solutions. Total volume was changed at least three times. Poly (2-acetamidoacrylic acid) used had a molecular weight of 19154 g/mol (M_n).

3.2.2 Synthesis of Aqueous 3-Mercaptopropionic Acid and Poly(AAA) Capped CdS QDs

30.0 mg of $Cd(CH_3COO_2)\cdot 2H_2O$ was dissolved in 200 mL of deoxygenated water in a three-necked round bottomed flask under continuous stirring and Argon flow. Desired amount of coating material P(AAA) or its mixture with 3-MPA was added to the cadmium containing solution and the pH was adjusted to 7.5. Then, 2.8 mg of $Na_2S.3H_2O$ was added to deoxygenated Cd-solution at room temperature. Reactions were carried out for 1 hour at 50°C under Argon. All QDs were stored in fridge. Before characterizations, all samples were prepared by multiple washing of QDs with water through Amicon ultrafiltration tubes (Amicon Ultra-15 Regenerated Cellulose 3000 MWCO) at 3800 rpm in order to remove excess organic materials or inorganic ions from solutions. Total volume was changed at least three times. Poly (2-acetamidoacrylic acid) used had a molecular weight of 19154 g/mol (M_n).

3.2.3 Characterization Techniques

Ultraviolet-Visible-Near Infrared (UV-Vis) and Photoluminescence (PL) spectra were recorded with a Schimadzu UV-Vis-NIR spectrophotometer model 3101 PC and Horiba Jobin Yvon-Fluoromax 3 spectrofluorometer, respectively. All optical measurements were performed at room temperature under ambient conditions. PL spectra of CdS QDs were recorded in the range 370 nm to 850 nm at a 5 nm interval at the excitation wavelength of 355 nm. A 370 nm filter was used for these measurements. PL spectra were all calibrated with respect to absorption values at the excitation wavelength. Quantum yields were estimated according to the reported procedures by diluting the samples to three different concentrations having max 0.1 absorbance at the excitation wavelength of 355 nm.[26] Rhodamine B was used as a reference (QY= 31% in water). Brus equation was used to calculate the sizes of nanoparticles.[27]

3.2.4 *In vitro* cell viability

Toxicity of quantum dots to mammalian cells was determined by colorimetric, enzyme-based assay using MTT for counting live cells. The assay is based on the reduction of 3-(4,5-dimethythiazol-2-yl)-2,5-diphenyl tetrazolium bromide (MTT) to insoluble, dark purple needle-shaped formazan product by mitochondrial succinate dehydrogenase. Since the reduction of MTT can occur only in metabolically active cells, the level of activity is a measure of the viability of the cells.

HeLa (human cervix adenocarcinoma epithelial cells) and MCF-7 (human breast adenocarcinoma epithelial cells) cell lines were used in the assay. Cells were cultured at a density of 5 x 10^4 in 96-well plates in 200µL DMEM medium supplemented with 10% FBS and 1% penicillin-streptomycin at 37°C, under 5% CO_2 for 24 hours. Then the medium was renewed and QDs were added at certain doses. Following 24 hours of incubation with QDs, cells were washed with CMF-PBS and 50µL of MTT reagent (5 mg/mL) was added to each well in new medium. The cells were incubated for 4 hours in CO_2 incubator. The insoluble purple formazan product was solubilized with DMSO:Ethanol (1:1) by gentle mixing of the plates for 15 minutes and then the absorbance was measured on a ELx800 Biotek Elisa reader at 600 nm, with reference at 630 nm. Viability of the cells was determined as the percentage viability of control cells which were not incubated with QDs. Results reported are averages of three experiments.

3.3 Results and Discussion

3.3.1 Properties of CdS Coated With P(AAA) and Cysteine/P(AAA) Mixed Coating

P(AAA) and its mixtures with cysteine were evaluated as a coating for CdS QDs. Influence of the coating composition on the particle size and luminescent properties were investigated at a fixed Cd^{2+}:S^{2-} ratio of 5.0, pH around 7.5 (before

sulfide addition) and at 50°C. Variations in the coating composition were done at a fixed COOH /Cd of 1.5 for P(AAA)/cysteine mole ratios of 100/0, 80/20, 60/40, 40/60, 0/100. All compositions supported well suspended CdS QDs with luminescent properties. All particles were luminescent in the visible range upon excitation with 365 nm (Figure 3.1). Particle properties are given in Table 3.1.

Table 3.1 Properties of QDs prepared at different mol% of cysteine and P(AAA).

Sample ID	Cystein[a] %	P(AAA)[b] %	Particle Size[c] (nm)	λ_{onset} (nm)	$\lambda_{PL\ max}$ (nm)	FWHM[d] (nm)	QY[e] %
CYS-100	100	0	2.2	358	481	156.0	3.6
CYS-80	80	20	2.2	358	490	145.4	17
CYS-60	60	40	2.5	397	511	163.1	14
CYS-40	40	60	2.6	400	516	165.2	53
CYS-20	20	80	3.2	444	542	209.8	35
CYS-0	0	100	4.3	480	698	-	3.6

[a]Mol% of COOH coming from cysteine in feed. [b]Mol% of COOH coming from P(AAA) in feed. [c]Calculated by Brus effective mass approximation.[27] [d]Full-width at half-maximum calculated from PL spectra. [e]QY calculated reported with respect to Rhodamine B reference.

Absorption onsets of all particles are at shorter wavelengths than 512 nm indicating quantum confinement (Figure 3.3, Table 3.1). QD crystals are between 2.2-4.3 nm. P(AAA) was demonstrated as an effective coating however, QDs coated with P(AAA) (CYS-0) are the biggest nanoparticles with relatively poor luminescence (3.6% QY) (Table 3.1).This is also accompanied with largest full-width at half maximum of the PL peak which does indicate greater particle size distribution. This is reasonable because as the size of the coating molecule increases, not only does the possibility of binding multiple Cd^{2+} increase (which increases the effective concentration within the clusters) but also the bridging between nanoparticles increases. Such an increase in the inter-particle interactions leads into the observed greater particle size distribution. Similar behavior was observed with poly (acrylic

acid)[28]. Macromolecules, fail to provide a dense coating on the particle surface due to the electrostatic repulsion of the neighbouring groups, steric crowding and backbone configuration, leaving trap sites which is detrimental for luminescent properties. This at least partially explains the low quantum yield for all P(AAA) coated CdS. Smaller complexes can be formed with cadmium which limits the amount of cadmium in a cluster and provide smaller particles. Cysteine coated CdS nanoparticles were the smallest particles (2.2 nm) luminescing blue. QDs prepared with mixed coating showed absorption onset and PL max between the CYS-0 and CYS-100 (Figure 3.3) with dramatically improved QY (between 14-53%). These values are quite high when compared to cysteine coated aqueous QDs in the literature.[28,29] Highest quantum yield of 53% was achieved at the coating compositions of 60/40 P(AAA)/cysteine. Actually, CdS with 100% to 40% cysteine in the coating were all between 2.2-2.5 nm and luminesce blue-green (Figure 3.1, Table 3.1). Only the CdS with 20% cysteine had yellow-green luminescence and showed a dramatic jump in the crystal size to 3.2 nm. These indicate a synergy originating from the use of small molecules and macromolecules together in the coating. Polymeric coatings usually provide a more stable surface coating which provide a greater colloidal stability. Incorporation of cysteine decreased the particle size, and probably trap sites.

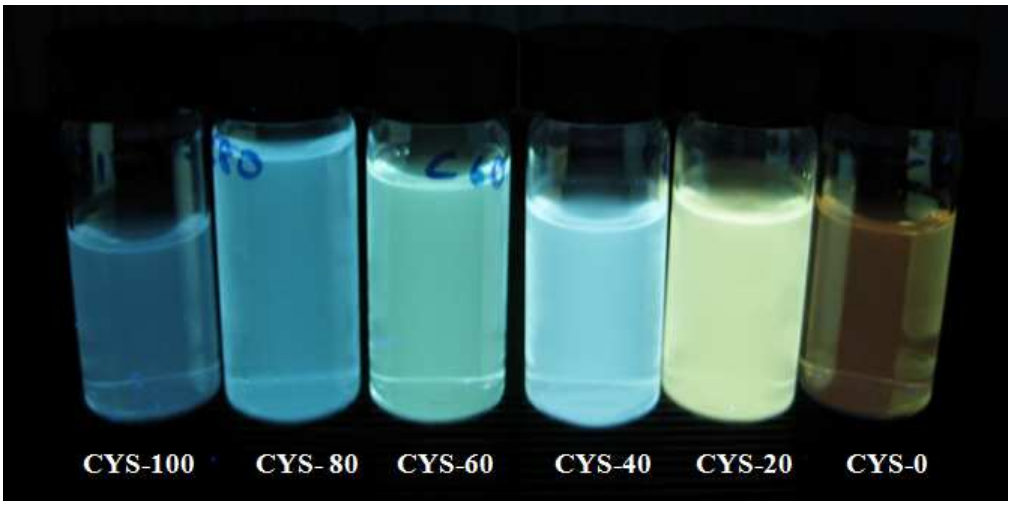

Figure 3.1 The photograph of aqueous CdS QDs under excitation at 365 nm. From left to right PAAA/Cysteine:0/100, 20/80, 40/60, 60/40, 100/0.

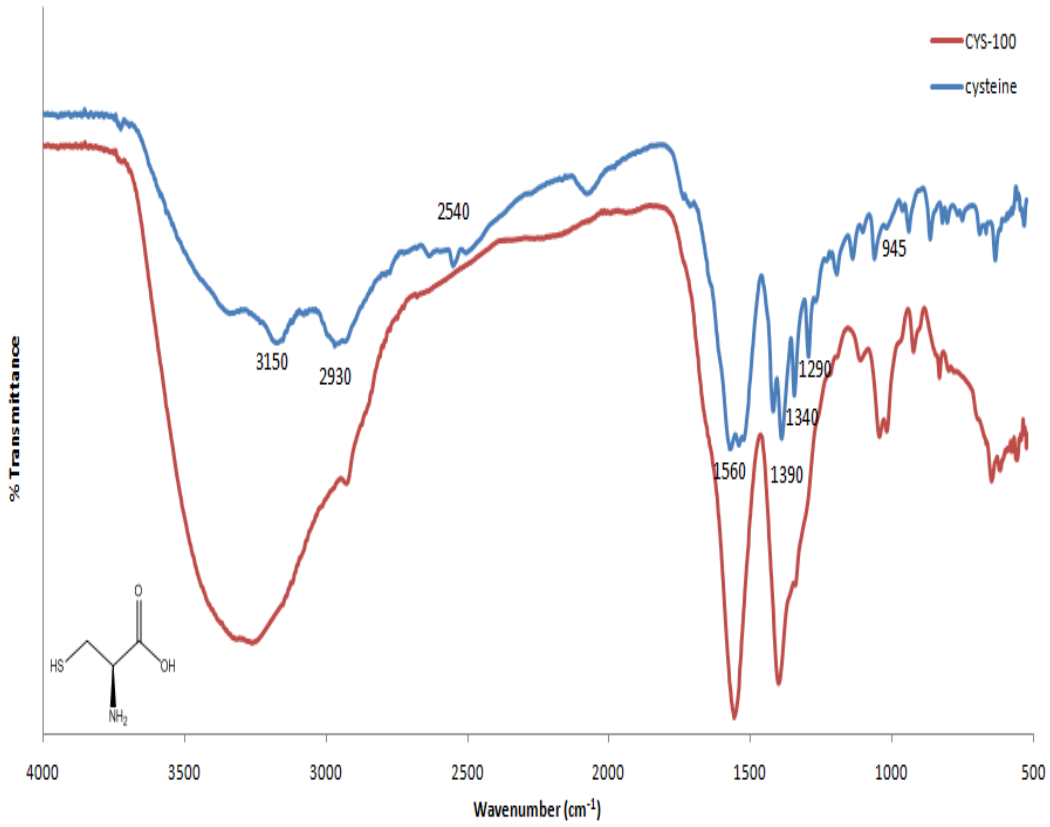

Figure 3.2 FT-IR spectra of washed CdS-Cysteine QDs and Cysteine.

FT-IR (Figure 3.2) spectra of the washed nanoparticles provided information about the cysteine coating. Binding from the thiol was confirmed by the disappearance of the thiol stretching and bending modes at 2540 and 945 cm^{-1}. Characteristic N-H and O-H stretching bands of cysteine are at 3150 cm^{-1}. C-H and NH_3^+ stretching peaks of cysteine appear at 2930 cm^{-1}. Broad peak between 3000-3500 cm^{-1} in FT-IR of washed CYS-100 QDs can be assigned to the asymmetric and symmetric stretching of $–NH_2$. Broadening can be attributed to the possible hydrogen bonding. Asymmetric and symmetric stretching modes of carboxylate are at 1560 and 1390 cm^{-1}. C-N stretching peak of cysteine appears at 1290 cm^{-1}.

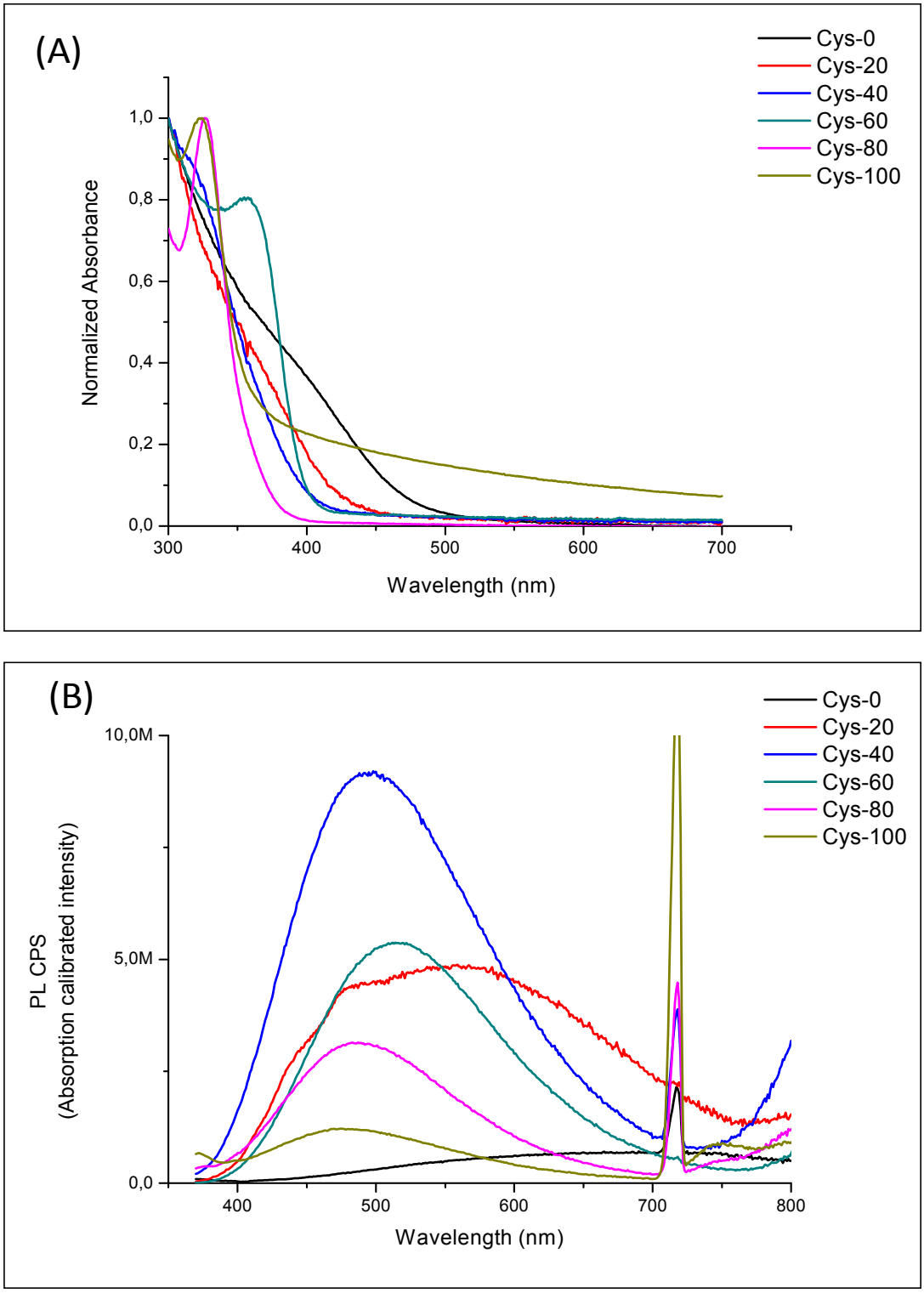

Figure 3.3 (A) Room temperature UV-Vis absorption spectra of washed CdS nanoparticles with varying mol% of cysteine and P (AAA) **(B)** Absorption calibrated PL spectra of washed CdS nanoparticles with varying mol% of cysteine and P (AAA).

3.3.2 Particle Stability

All washed samples were stored in the refrigerator and after several days the stability of CdS QDs was investigated. Particles are quite stable both optically and colloidally (Table 3.2 and Figure 3.4). Optical properties and stability is influenced dramatically by the surface quality. CYS-60 although originally did not possess the highest QY showed no reduction after being stored for 10 days indicating possibly the best composition for stability. CYS-40 which had the 53% (highest) QY showed only 23% drop but CYS-20 which was the largest of the particles with the mixed coating showed the greatest drop with 83% with a slight reduction in size as well. Size reduction may originate from the oxidation at the surface. Reasons behind the loss of luminescence may be various. Mostly detachment of coating through oxidation or protonation causes trap sites, which may at long run bring together precipitation as well.

Table 3.2 Properties of QDs after 10 days in the refrigerator.

Sample ID	Cysteine [a] %	P(AAA) [b] %	Particle Size[c] (nm)	λ_{onset} (nm)	$\lambda_{PL\ max}$ (nm)	FWHM [d] (nm)	QY[e] %
CYS-100	100	0	2.2	361	488	164.9	-
CYS-80	80	20	2.2	367	492	146.5	22
CYS-60	60	40	2.6	398	514	160.6	16
CYS-40	40	60	2.4	382	497	170.6	46
CYS-20	20	80	2.9	425	553	262.9	43
CYS-0	0	100	4.3	482	703	-	-

[a]Mol% of cysteine in feed. [b]Mol% of P(AAA) in feed. [c]Calculated by Brus effective mass approximation.[27] [d]Full-width at half-maximum calculated from PL spectra. [e]QY calculated by using Rhodamine B as a reference.

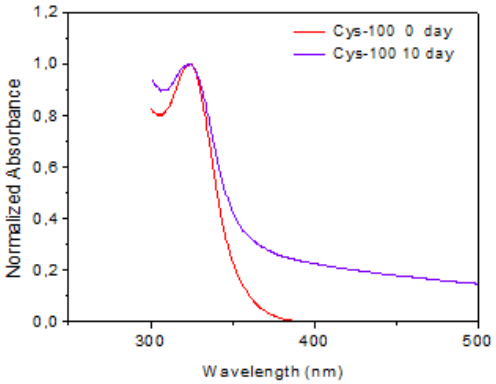
Cys-100 0 day
Cys-100 10 day
Normalized Absorbance
Wavelength (nm)

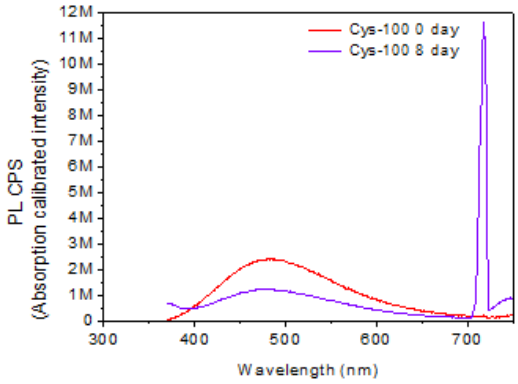
Cys-100 0 day
Cys-100 8 day
PL CPS
(Absorption calibrated intensity)
Wavelength (nm)

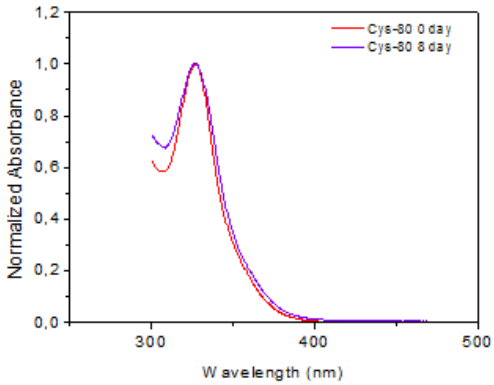
Cys-80 0 day
Cys-80 8 day
Normalized Absorbance
Wavelength (nm)

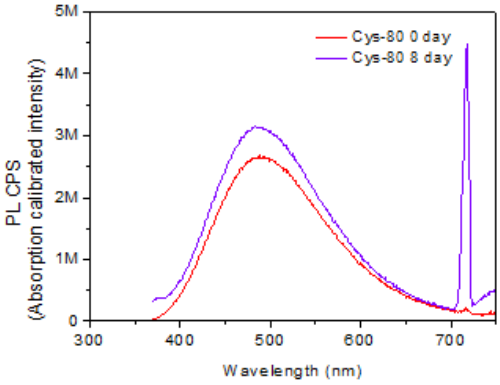
Cys-80 0 day
Cys-80 8 day
PL CPS
(Absorption calibrated intensity)
Wavelength (nm)

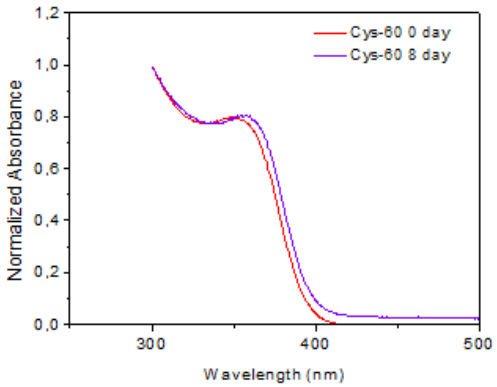
Cys-60 0 day
Cys-60 8 day
Normalized Absorbance
Wavelength (nm)

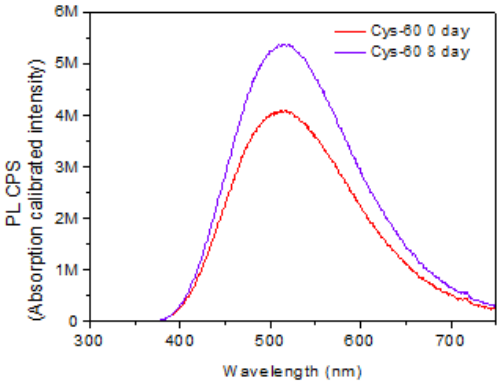
Cys-60 0 day
Cys-60 8 day
PL CPS
(Absorption calibrated intensity)
Wavelength (nm)

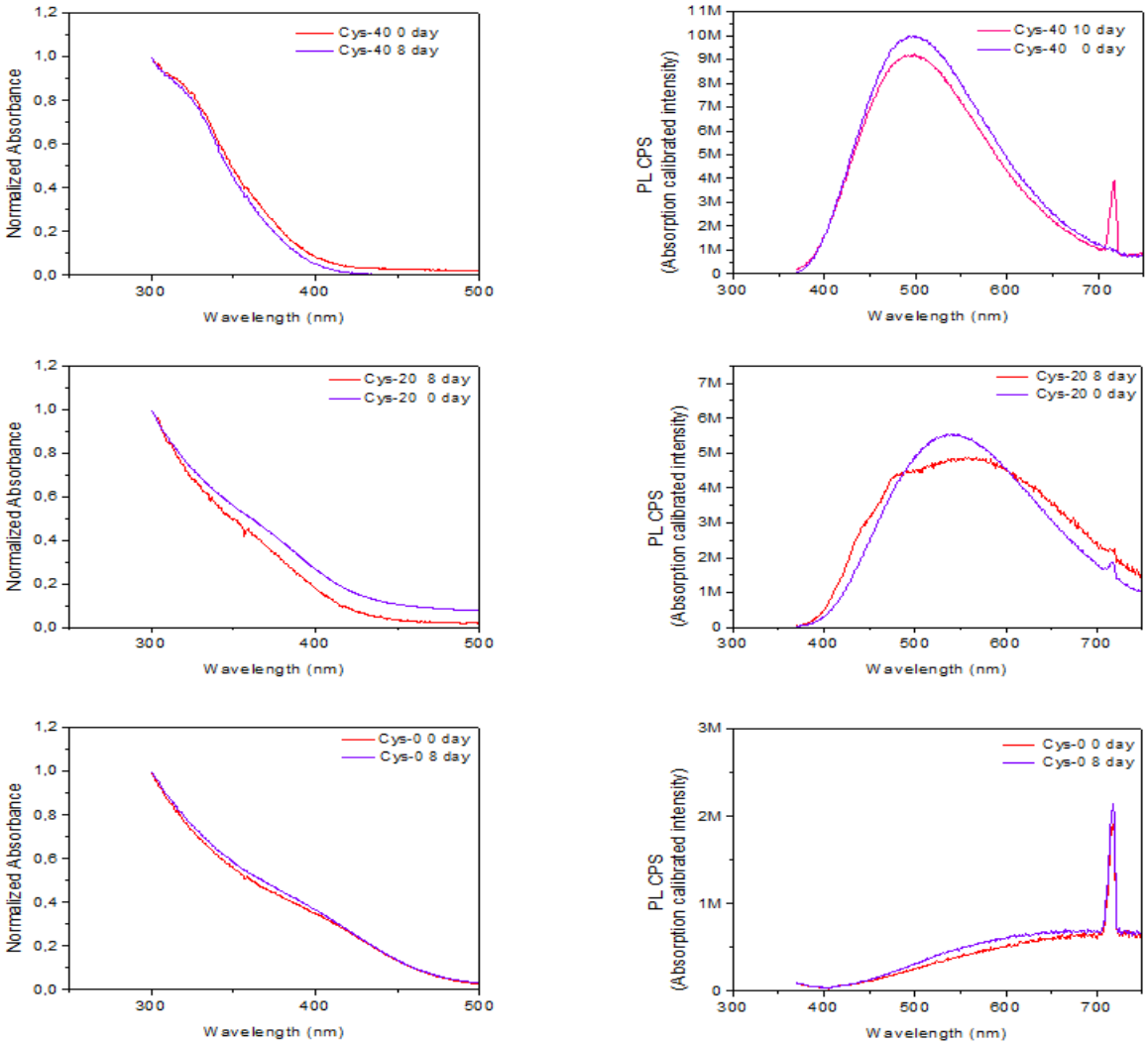

Figure 3.4 The absorption and normalized PL spectra of washed CdS nanoparticles with varying mol% of cysteine and P (AAA) stored in refrigerator after several days (λ_{exc}=355nm).

3.3.3 Influence of pH On Particle Properties

Since the coating molecules have pH sensitive nature, luminescence of the CdS QDs at different pH values was investigated. CdS with the coating compositions of 60/40 P(AAA)/cysteine was adjusted to 6 and 10. The original washed sample had a pH of 7.55.

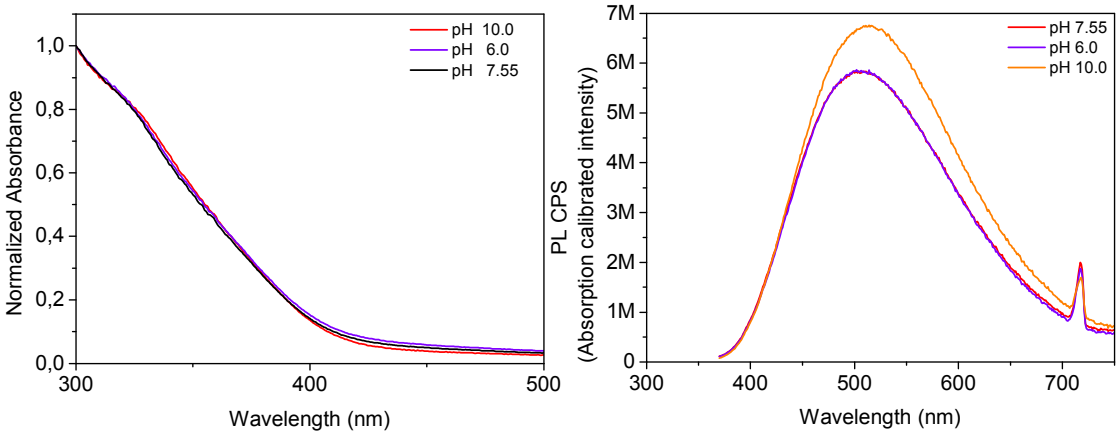

Figure 3.5 The absorption and normalized PL spectra of washed CdS nanoparticles at different pH values (λ_{exc}=355nm).

Table 3.3 Properties of washed CdS QDs (P(AAA)/Cysteine = 60/40) at different pH.

Sample ID	Particle Size[c] (nm)	λ_{onset} (nm)	$\lambda_{PL\ max}$ (nm)	FWHM[d] (nm)
pH 10.0	2.6	404	513	182.7
pH 6.0	2.6	404	503	181.6
pH 7.55	2.6	404	503	180.6

[c]Calculated by Brus effective mass approximation.[27] [d]Full-width at half-maximum calculated from PL spectra.

Changing the final pH of the QDs resulted in no significant change in the UV-Vis absorption spectra of CdS nanoparticles. In addition, PL intensity and PL max (503 nm) of samples at pH 7.55 and 6.0 was identical. However, at the pH 10.0 the PL intensity is increased and the PL max value (513 nm) shifted to a slightly higher value. Although QY of these nanoparticles was not calculated, from the intensity of PL spectra and increase in the λ PL max we can conclude that increasing the pH resulted in an increase in the QY and a slightly larger crystal size. These results can be explained by several things. A possible explanation for the improved luminescence

efficiency in alkaline medium can be the formation of $Cd(OH)_2$ at defect sites, which in a way act like a core-shell particle, decreasing non-radiative decay. Since at pH 6, carboxylates are not protonated yet, there was no significant difference in the particle properties. This indicates that particles can be used safely in the pH range of 6-10.

3.3.4 Effects of COOH/Cd Ratio On The Particle Size And Optical Properties

Coating has multiple duties in the preparation of QDs. Adsorption on the growing crystal surface is one of the most influential ways to passify the surface and control the crystal size. Influence of the increasing coating amount from COOH/Cd 1.5 to 3 on the particle size and luminescent properties was investigated at the coating compositions of 60/40 P(AAA)/cysteine under identical synthetic conditions (pH 7.5 and 50°C). This brought about a blue shift in the UV and PL indicating a smaller size crystal with increasing amount of the coating. Coating molecules form complexes with Cd^{2+} prior to addition of S^{2-} and increasing the coating amount decreases the free cadmium ions in the solution, allowing more homogenous nucleation and growth.[29] This can also lead into narrower full-width at half maximum of the PL peak which does indicate smaller particle size distribution. On the other hand, cysteine can prevent the growth through thiol binding competing with S^{2-}. An important benefit of increasing the coating amount is the enhanced luminescence of QDs. Addition of only twice as coating material (COOH/Cd=3) provided more than 150% improvement in quantum yield (Table 3.4). It also provided a slight narrowing of the PL peak along with smaller crystal sizes. Therefore, impact of the amount of ligand to cadmium ratio on luminescent properties is very crucial since quantum yield depends on many things such as effectiveness of the capping and surface quality. Effective surface passivization is critical for optical properties of quantum dots.

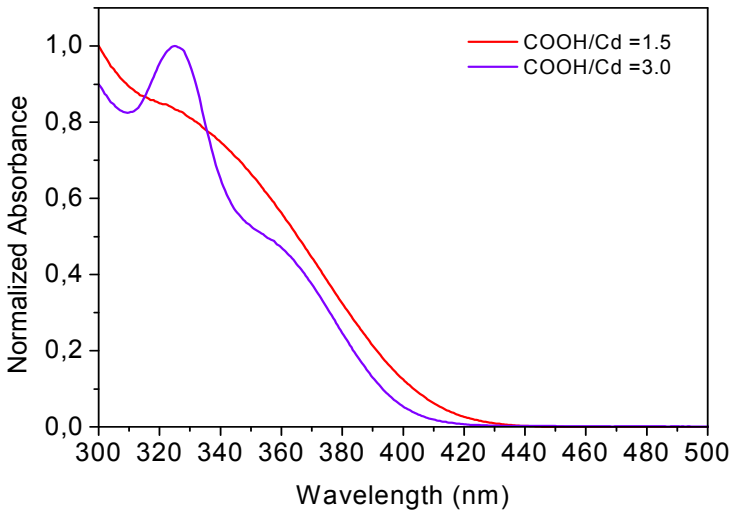

Figure 3.6 UV-Vis absorption spectra of washed CdS nanoparticles (P(AAA)/Cysteine = 60/40) with different COOH/Cd ratio.

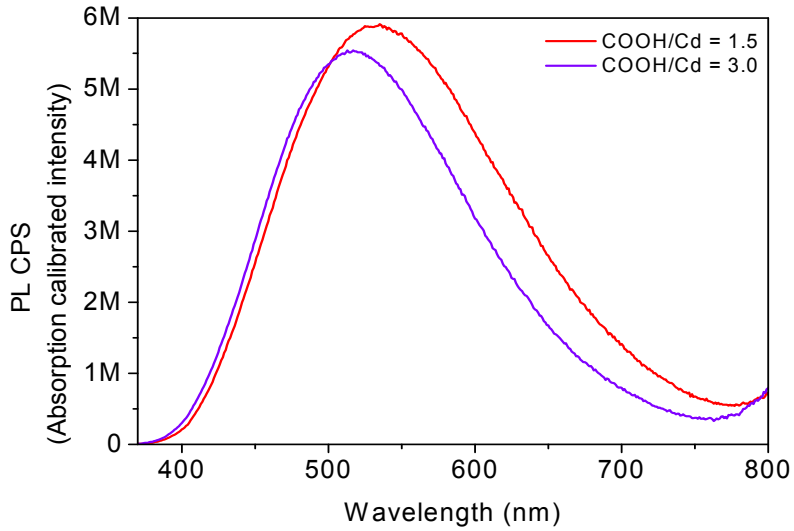

Figure 3.7 Absorption calibrated PL spectra of washed CdS nanoparticles with varying COOH/Cd (λ_{exc}=355nm).

Table 3.4 Properties of washed CdS (P(AAA)/cysteine = 60/40) nanoparticles with varying COOH/Cd ratio.

COOH/Cd	Particle Size[c] (nm)	λ_{onset} (nm)	$\lambda_{PL\ max}$ (nm)	FWHM[d] (nm)	QY[e]%
1.5	2.7	410	588	186.7	20
3.0	2.6	400	554	162.0	53

[a]Mol ratio. [b]Mol% of COOH coming from P(AAA) in feed. [c]Calculated by Brus effective mass approximation[27]. [d]Full-width at half-maximum calculated from PL spectra. [e]QY calculated by using Rhodamine B as a reference.

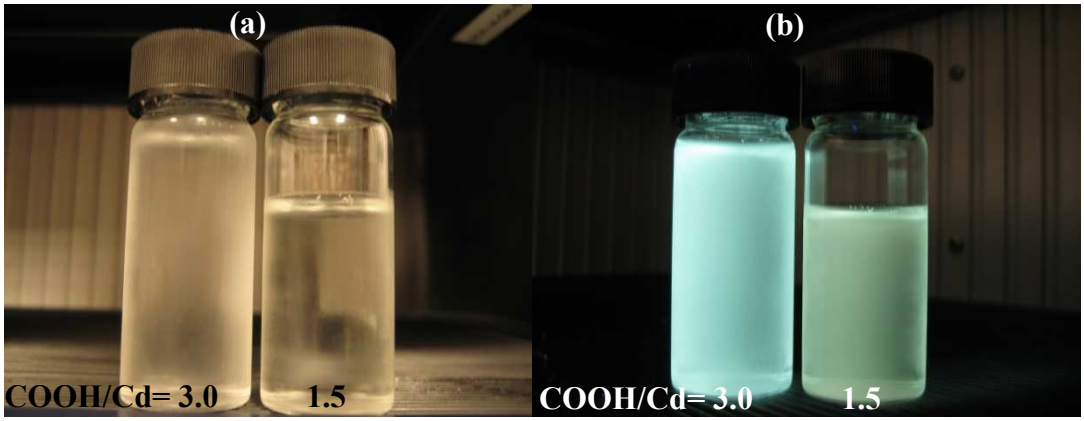

Figure 3.8 Pictures of the P(AAA)/Cysteine (60/40)-CdS nanoparticles under (a) daylight and (b) UV excitation (λ_{exc}) 366 nm.

3.3.5 Influence of Reaction Temperature on Particle Properties

Influence of the reaction temperature on the particle size and luminescent properties were investigated at the following synthetic conditions: coating compositions of 60/40 P(AAA)/cysteine, pH 7.5, COOH/Cd ratio of 3 and Cd/S ratio of 2. Reactions were carried out at 50°C and room temperature. Reaction temperature has a dramatic effect on particle size and the color of emission. Major growth is

originating from Ostwald ripening process which refers to the growth of larger crystals in the expense of smaller ones that have higher solubility than the larger ones. As the temperature increase the magic size of the crystal (which is stable at that temperature) increases. This causes an increase in the particle size with relatively larger size distributions. Increasing the reaction temperature brought about a red shift in the UV and PL indicating a greater size crystal. Table 3.5 shows larger FWHM at elevated reaction temperature as well, confirming Ostwald ripening process. PL spectra showed about 22 % decrease in PL intensity with decreasing temperature. Increasing reaction temperature may increase the adsorption – desorption of capping agents from the surface, and decrease the stability of the quantum dots favoring the nucleation and growth which may also cause the loss of coating from the surface creating defects that are detrimental for a strong luminescence.[28,29] Previously, our group studied the influence of reaction temperature on the luminescence properties of the poly (acrylic acid) –mercaptoacetic acid capped CdS quantum dots.[28] It was found that the influence of the reaction temperature on the quantum yields of the CdS quantum dots are dramatically different for the two types of coatings. QY of the poly (acrylic acid) coated CdS quantum dots were low (7-8%) but did not change with the reaction temperature. However, QY of the mercaptoacetic acid coated CdS nanoparticles decreased from 43.6% to 1.6% as the reaction temperature was increased from 30 to 90°C. Also, cysteine coated CdS QDs showed about 30% decrease in QY as the temperature increased from 30 to 60°C.[29] This was related to the multidentate binding and low mobility of polymers at high reaction temperatures compared to more mobile and small mercaptoacetic acid. Also, mixed coatings showed less sensitivity to temperature as we have seen here. However, increasing the reaction temperature leads to an increase in the luminescence of the quantum dots in our case which is not very usual at such reactions. Higher temperatures may lead into better crystallization but this usually requires much higher temperatures. The origin of such behavior requires further study.

Table 3.5 Properties of washed CdS nanoparticles at different reaction temperatures.

Temperature (°C)	Cysteine[a] %	P(AAA)[b] %	Particle Size[c] (nm)	λ_{onset} (nm)	$\lambda_{PL\ max}$ (nm)	FWHM[d] (nm)
R.T.	40	60	2.4	384	506	158.2
50	40	60	2.6	400	516	165.2

[a]Mol% of cysteine in feed. [b]Mol% of P(AAA) in feed. [c]Calculated by Brus effective mass approximation.[27] [d]Full-width at half-maximum calculated from PL spectra.

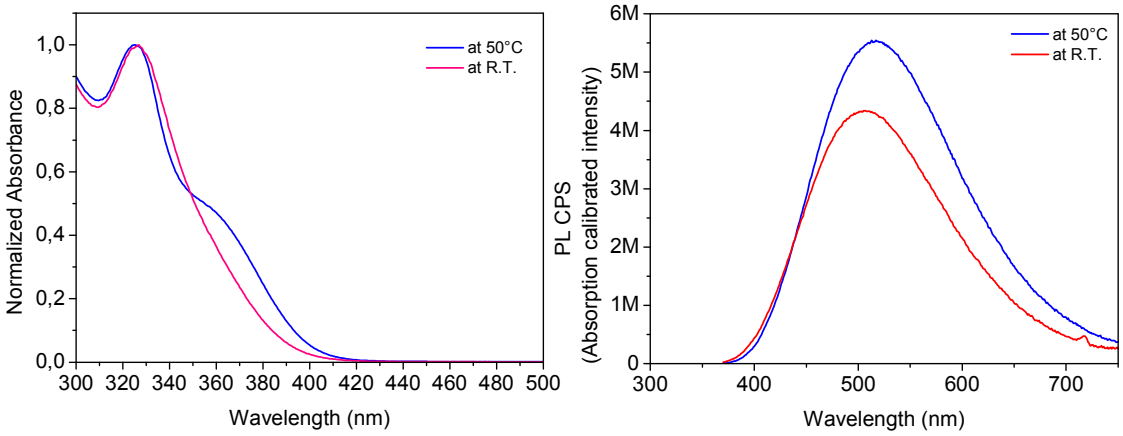

Figure 3.9 The effect of reaction temperature on the absorption and normalized PL spectra of washed CdS nanoparticles (λ_{exc}=355nm)

3.3.6 Properties of CdS Coated With Poly (AAA) and 3MPA/Poly (AAA) Mixed Coating

Influence of the coating compositions of 100/0, 80/20, 60/40, 40/60, 0/100 P(AAA)/3-mercaptopropionic on the particle size and luminescent properties were investigated at a fixed Cd^{2+}:S^{2-} ratio of 5.0, pH 7.5. COOH /Cd ratio of 1.5 and reaction temperature of 50°C.

Table 3.6 Properties of QDs prepared at different mol% of 3MPA and P(AAA).

Sample ID	3MPA[a] %	P(AAA)[b] %	Particle Size[c] (nm)	λ_{onset} (nm)	$\lambda_{PL\ max}$ (nm)	FWHM[d] (nm)
3MPA-100	100	0	2.1	353	533	184.6
3MPA-80	80	20	2.1	345	526	185.3
3MPA-60	60	40	2.1	351	508	170.3
3MPA-40	40	60	2.1	354	539	194.8
3MPA-20	20	80	3.1	434	572	205.2
3MPA-0	0	100	4.1	476	624	-

[a]Mol% of 3MPA in feed. [b]Mol% of P(AAA) in feed. [c]Calculated by Brus effective mass approximation.[27] [d]Full-width at half-maximum calculated from PL spectra.

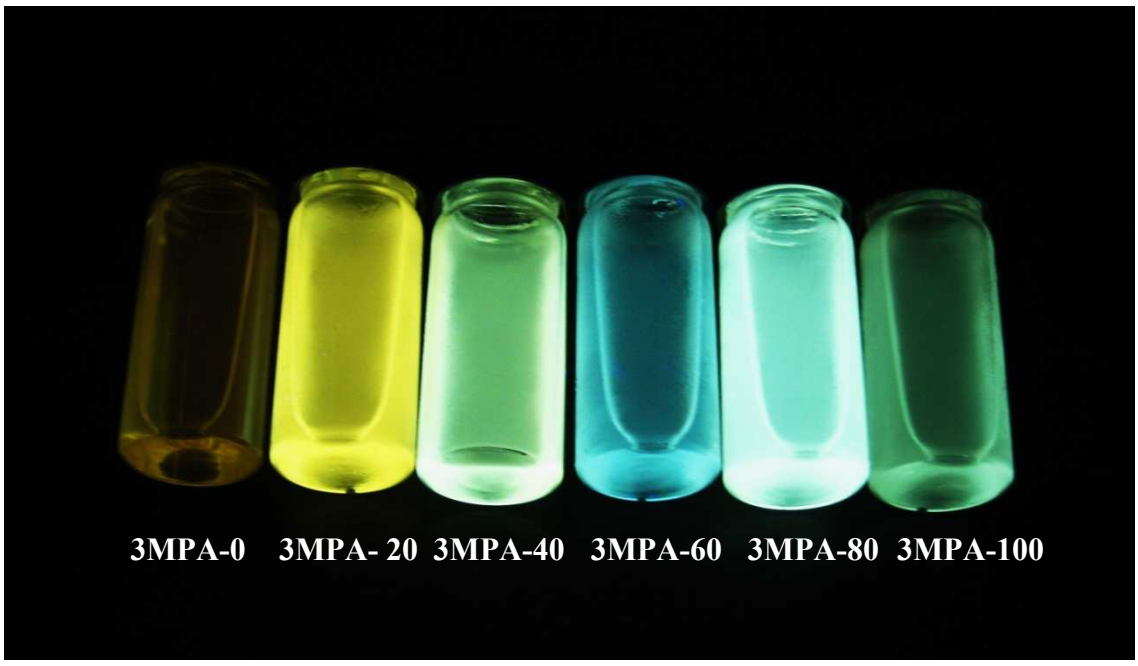

Figure 3.10 The photograph of aqueous CdS QDs under UV excitation at 365 nm.

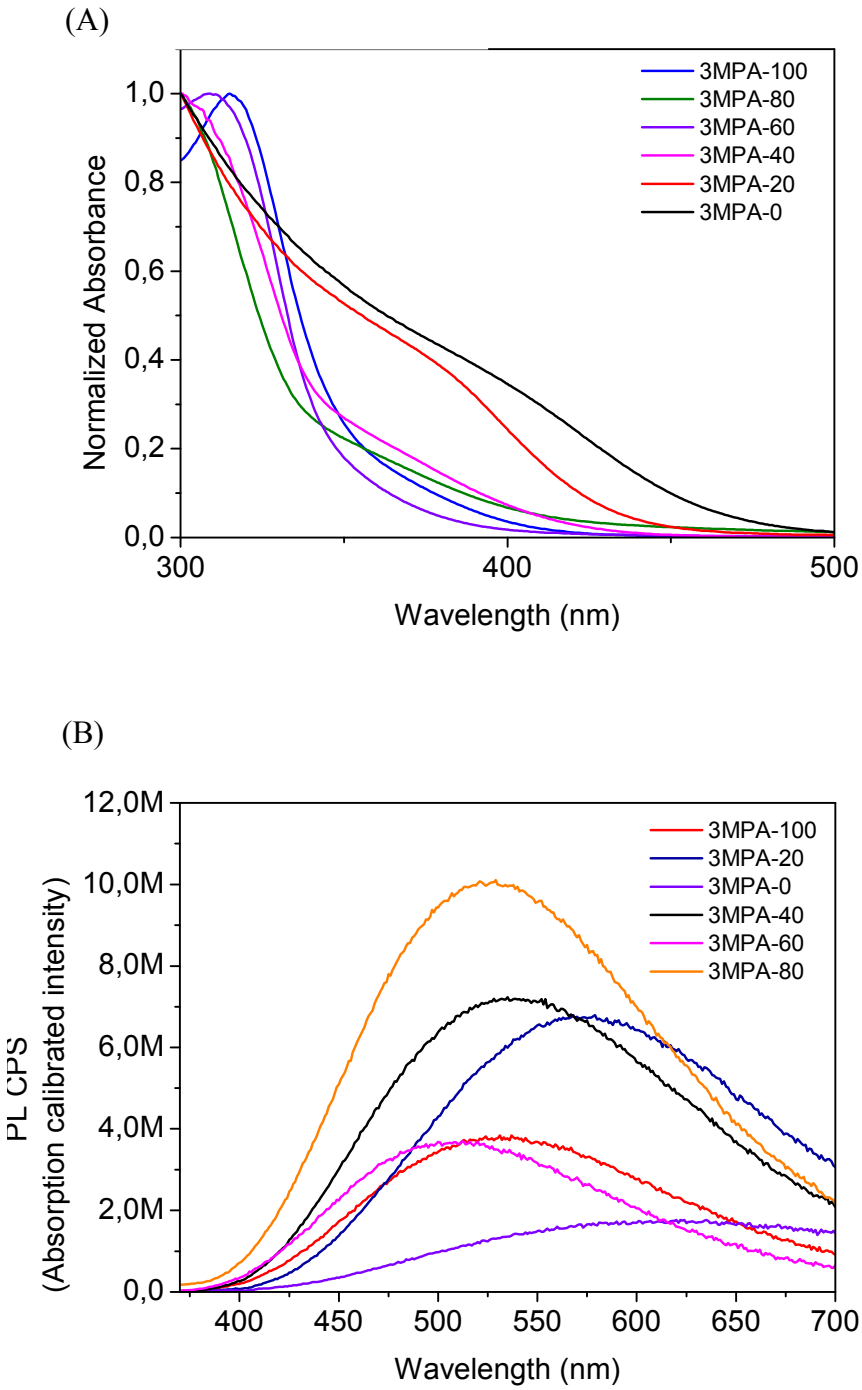

Figure 3.11 (A) Room temperature UV-Vis absorption spectra of washed CdS nanoparticles with varying mol% of 3-MPA and P (AAA) **(B)** Absorption calibrated PL spectra of washed CdS nanoparticles with varying mol% of 3-MPA and P (AAA).

All compositions supported well suspended CdS QDs that are luminescent in the visible range (Figure 3.11). Crystal sizes calculated by Brus equation were in the range of 2.1-4.1 nm (Table 3.6). CdS nanoparticles coated with P(AAA) (3MPA-0) had largest crystal size and broadest size distribution than the 3MPA and 3MPA-P(AAA) coated CdS quantum dots, just as in the case of P(AAA)-cysteine coated particles. However, this coating mixture provided a more colorful portfolio than P(AAA)-cysteine, meaning particles luminescing in different colors. QDs with emission from green to orange were obtained. Nanoparticles with the binary coating had smaller crystal sizes with narrower size distributions and comparable or much better luminescence than corresponding CdS nanoparticles coated with only P(AAA) or 3MPA (Table 3.6) indicating again a synergy originating from the mixed coating. At 80% P(AAA) particle size is dominated more by the macromolecule producing the second largest particles but luminescence was improved by the small amount of 3MPA, improving the luminescence about 5 times compared to CdS-P(AAA) (Figure 3.11). Best composition under this synthetic conditions is 20/80 P(AAA)/3MPA which increased the PL intensity about 2.5 times over CdS/3MPA.

3.3.7 Particle Stability

Stability of the washed particles were checked after three months of storage in the fridge. 3MPA-100 showed the highest PL intensity reduction. A clear red shift of the absorption onset and PL max of the 3MPA-100 may originate from the oxidation of the surface at unpassivated sites because thioalkyl acid ligands such as 3MPA are able to form only a thin barrier around the quantum dots or hydrolysis of thiol bonds formed at the surface of the quantum dots.[30] Aldana and coworkers revealed that photochemical instability of 3MPA coated CdSe nanoparticles by H^1 NMR coupled with UV-Vis absorption.[30] The results show that the nanoparticles act as a catalyst for the oxidation so that surface thiols form disulfides and if the disulfides were soluble in water, nanoparticles precipitate due to the loss of surface passivation.[30] However, the

presence of excess free thiol ligands may replace the place that oxidized disulfides left and provide the solubility of QDs in water.[30] Also, possible release of sulfur may lead into deposition on the nanoparticle surface and hence an increase in the particle size. 3MPA-80 possesses the highest QY and showed almost no reduction in PL intensity after being stored three months indicating the best composition for stability. 3MPA-60, 3MPA-40 and 3MPA-20 showed a slight increase in size and full-width at half-maximum which is reasonable because of the possibility of the bridging between nanoparticles through macromolecules. The inter-particle interactions lead into the greater particle size distribution.

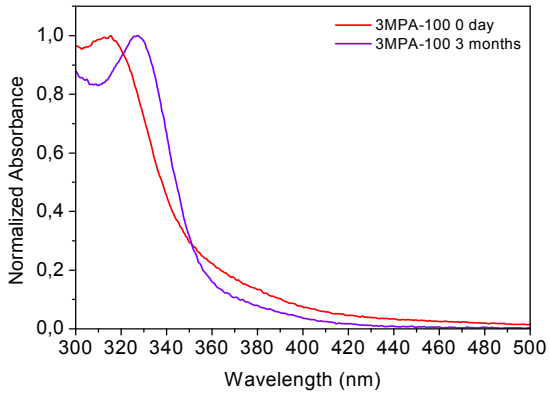

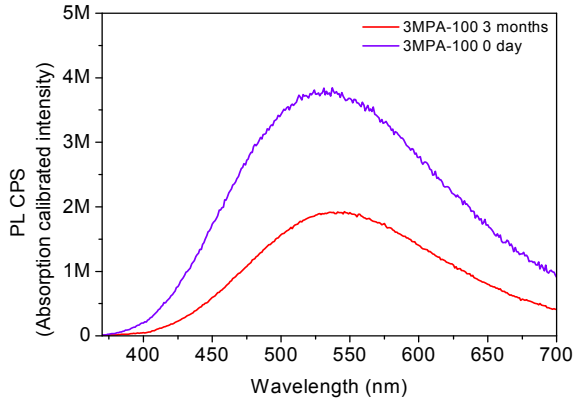

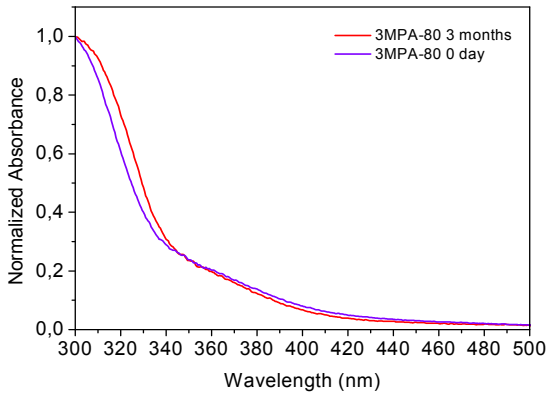

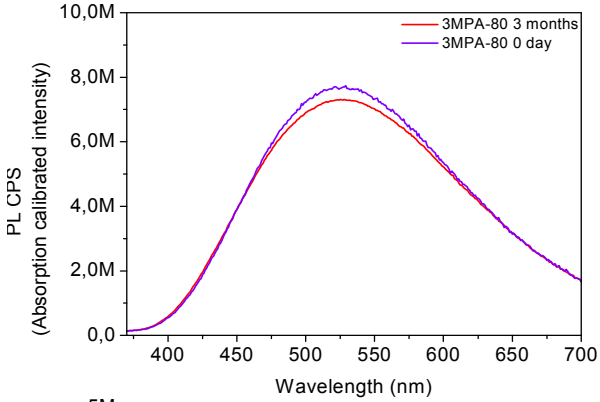

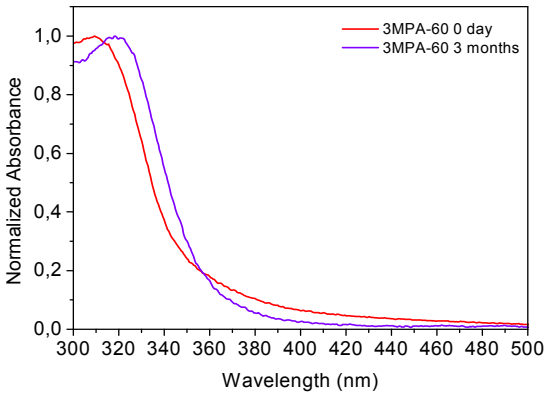

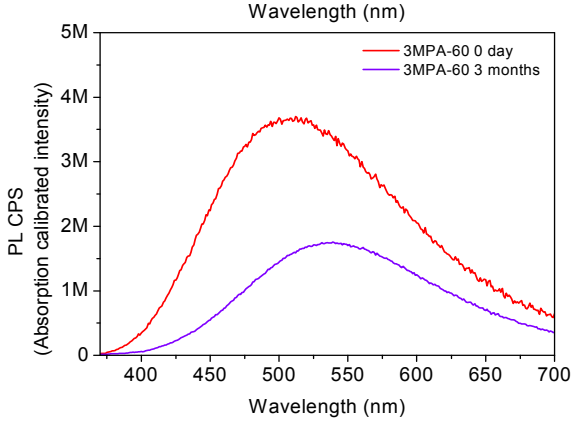

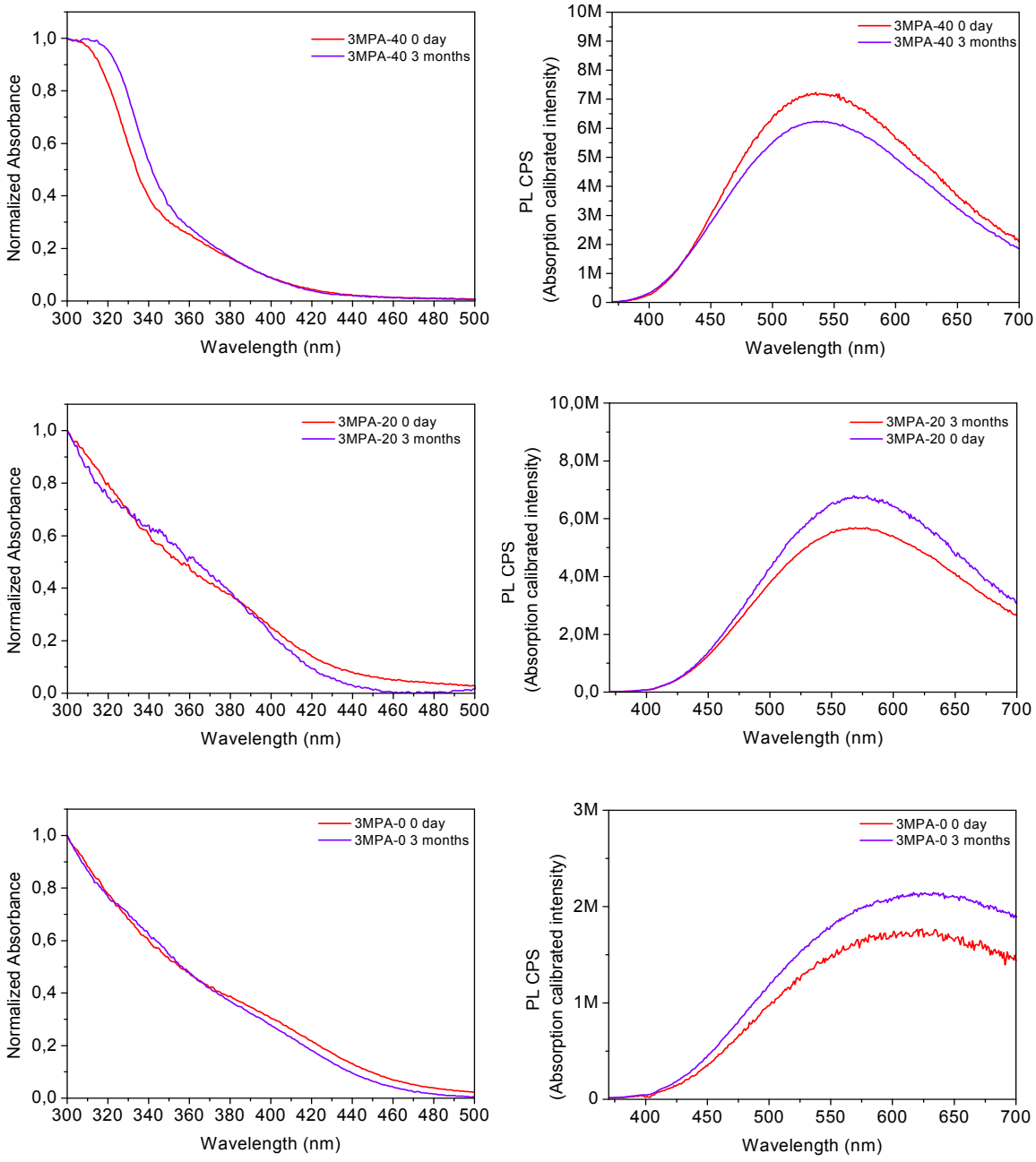

Figure 3.12 Absorption calibrated PL spectra of washed CdS nanoparticles with varying mol% of 3MPA and P (AAA) (λ_{exc}=355nm).

Table 3.7 Properties of QDs prepared at different mol% of 3MPA and P(AAA) after 3 months in the refrigerator.

Sample ID	3MPA[a] %	P(AAA)[b] %	Particle Size[c] (nm)	λ_{onset} (nm)	$\lambda_{PL\ max}$ (nm)	FWHM[d] (nm)	QY[e] %
3MPA-100	100	0	2.1	355	539	165.4	53.18
3MPA-80	80	20	2.1	349	528	190.1	56.66
3MPA-60	60	40	2.2	358	538	165.6	16.70
3MPA-40	40	60	2.2	361	540	198.0	18.12
3MPA-20	20	80	3.1	435	568	209.9	11.65
3MPA-0	0	100	3.6	459	626	-	11.75

[a]Mol% of COOH coming from 3MPA in feed. [b]Mol% of COOH coming from P(AAA) in feed. [c]Calculated by Brus effective mass approximation[27]. [d]Full-width at half-maximum calculated from PL spectra. [e]QY calculated by using Rhodamine B as a reference.

3.3.8 *In vitro* cell viability

3.3.8.1 *In vitro* cell viability of CdS Coated With Poly (AAA) and Cysteine/Poly (AAA) Mixed Coating

Although quantum dots are promising fluorophores in biomedical imaging, in *vivo use* of quantum dots is debated due to the important concern of toxicity. The primary reason of cytotoxity is the release of cadmium ions which bind to thiol groups on critical molecules in mitochondria and induce harm and damage,causing significant cell death.[20,31] Therefore, effective surface passivization is very crucial for quantum dots to become biologically inert. In addition, coating molecule should not cause any toxicity as well. However, the toxicity of quantum dots may also arise from other

reasons that do not depend on the components or coatings used. In mitochondria, the transfer of absorbed energy to nearby oxygen molecules by quantum dots induce reactive oxygen species (ROS) production such as free radicals (hydroxyl radical $^{\cdot}OH$ and superoxide $^{\cdot}O_2^-$ and singlet oxygen ($^1O_2$)),causing cell damage and death.[31]

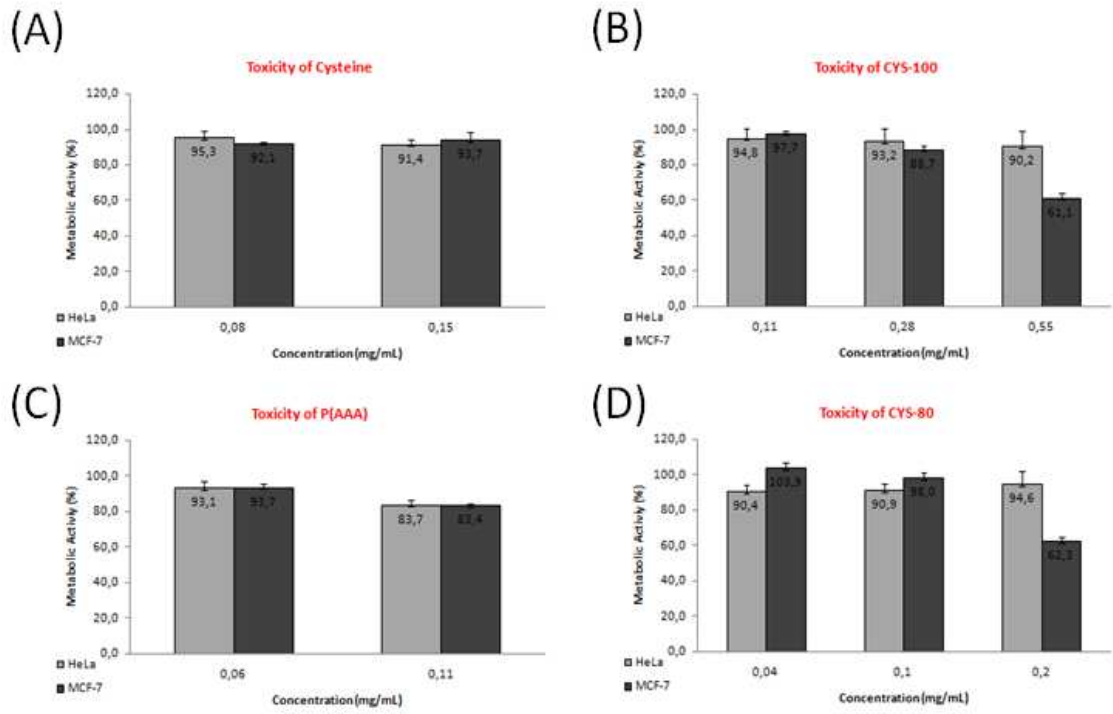

Figure 3.13 In vitro cell viability of cysteine, P(AAA) and CdS nanoparticles with varying 100 mol% of cysteine and P(AAA).

Cysteine is an advantageous coating for a QD for biological applications because it is biocompatible and non-immunogenic. Since poly (2-acetamidoacrylic acid) is a derivative of a dehydroalanine which is an uncommon amino acid, poly (2-acetamidoacrylic acid) may have a potential in biomedical applications. In order to evaluate the cytotoxicity of the novel QDs synthesized in this research, first, toxicity of the coating materials was evaluated. Viability of MCF-7 and HeLa cells in the presence of cysteine (0.08-0.15 mg/ml) is around 92-95%. In the presence of poly (2-acetamidoacrylic acid), at the low dose (0.06 mg/mL) viability is around 93% but at the high dose (0.11 mg/mL) viability decreased around 84%. Therefore, these results

show that poly (2-acetamidoacrylic acid) is a promising candidate for providing biocompatible, non-toxic coating. However, regardless of the cell line, cytotoxicity of cysteine is slightly a better than poly (2-acetamidoacrylic acid).

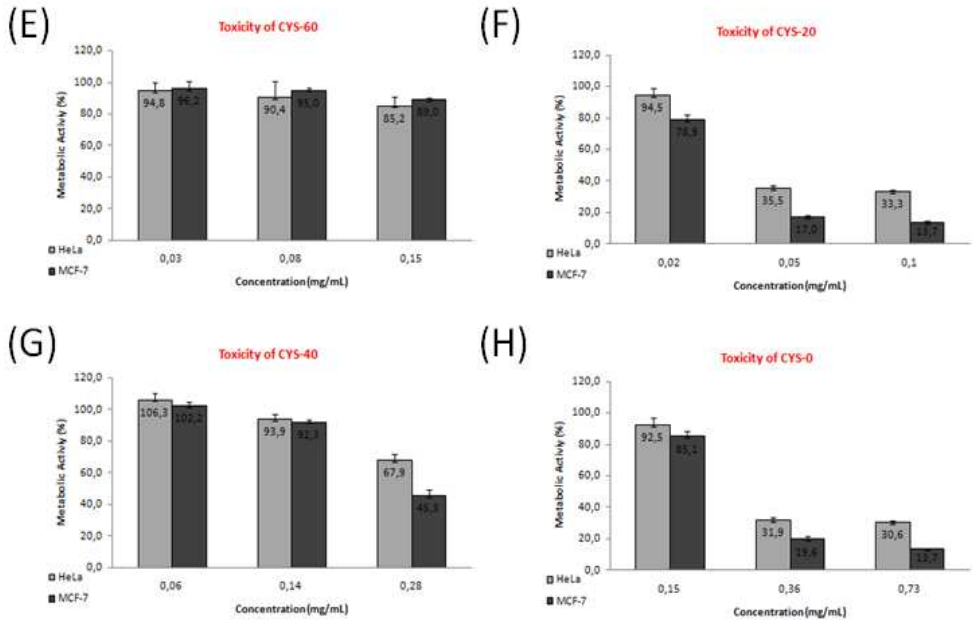

Figure 3.14 In vitro cell viability of CdS nanoparticles with varying mol% of cysteine and P(AAA).

Viability of MCF-7 and HeLa cells in the presence of CdS nanoparticles with varying mol% of cysteine and poly (2-acetamidoacrylic acid) can be seen in Figure 3.14. At the dose of 0.11 mg/mL, viability of HeLa and MCF-7 cells in the presence of CYS-100 (CdS nanoparticles coated with cysteine) is 94.8% and 97.7%. At nearly same dose level (0.1 mg/mL), in the presence of CYS-80 viability of HeLa cells drops to 90.9% and viability of MCF-7 cells is almost the same (98.0%) compared to CYS-100. As the cysteine amount in the coating decreases from 100% to 80%, viability of HeLa cells has dropped 4% . The toxicity difference between two QDs is significant at higher dose levels. For instance, the viability of MCF-7 cells at 0.55 mg/mL CYS-100 is 61.1% but even at smaller dose level of 0.2 mg/mL CYS-80 the viability is 62.3%, meaning that CYS-100 is less toxic to MCF-7 cells. This is reasonable because

cytotoxicity of cysteine is a better than poly (2-acetamidoacrylic acid). At the same dose level (0.14 mg/mL), regardless of the cell line cytotoxicity of CYS-40, QD that has the best optical properties is comparable with cysteine. Biocompatibility of QDs gets worse as the cysteine amount in the coating decreases dramatically. At dose level of 0.1 mg/mL, in the presence of CYS-80 the viability of MCF-7 and HeLa cells are 90.9% and 98.0%, respectively. However, at the same dose level of CYS-20 the viability of MCF-7 decreases by 63% and viability of HeLa cells decreases by 86%.

3.3.8.2 *In vitro* cell viability of CdS Coated With P(AAA) and 3MPA/P(AAA) Mixed Coating

In vitro cell viability of 3MPA, P(AAA) and CdS nanoparticles coated with P(AAA) and 3MPA/P(AAA) was evaluated in HeLa cells. First, toxicity of the coating materials was evaluated. Viability of HeLa cells in the presence of 3MPA (0.055-0.11 mg/ml) is around 80-88%. In the presence of poly (2-acetamidoacrylic acid), at the low dose (0.055 mg/mL) viability is around 93% but at the high dose (0.11 mg/mL) viability decreased around 84%. Cytotoxicity of poly (2-acetamidoacrylic acid) is better than the widely used 3MPA. Viability of HeLa cells in the presence of CdS nanoparticles with varying mol% of 3MPA and poly(2-acetamidoacrylic acid) can be seen in Figure 3.15. There is a dramatic toxicity difference between coating materials. For instances, at the same dose of 0.03 mg/ml, viability of HeLa cells in the presence of 3MPA-100 (CdS nanoparticles coated with 3MPA) is 74.2% but in the presence of 3MPA-0 (CdS nanoparticles coated with poly(2-acetamidoacrylic acid) is 100%. All particles except 3MPA-40 showed no significant cytotoxicity unlike pure 3MPA or pure P(AAA) coated particles. Therefore, these results show that poly (2-acetamidoacrylic acid) is a promising candidate for providing biocompatible, non-toxic coating and mixture of P(AAA) and 3MPA brings about a synergy in the toxicity as well.

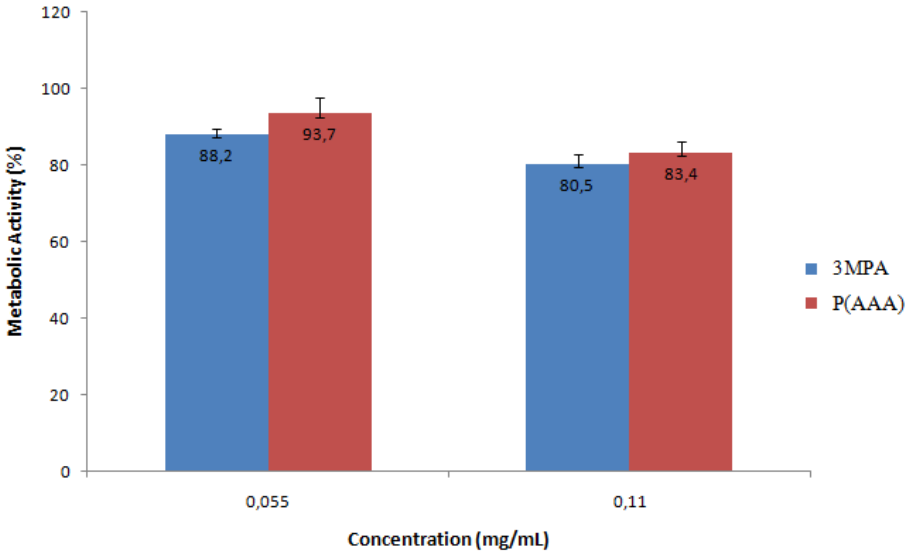

Figure 3.15 *In vitro* cell viability of 3MPA and P(AAA) in HeLa.

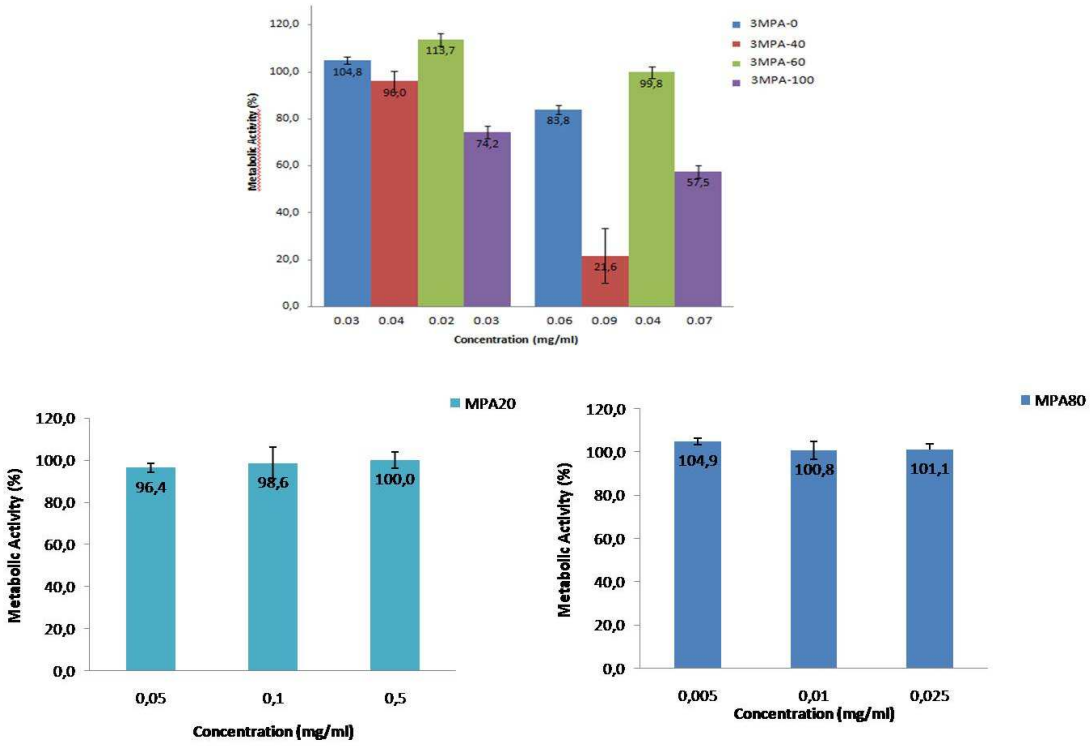

Figure 3.16 *In vitro* cell viability of CdS nanoparticles with varying mol% of 3MPA and P (AAA).

3.4 Conclusions

Poly(2-acetamidoacrylic acid) (P(AAA)) has been shown as an effective and biocompatible coating for stable aqueous CdS QDs for the first time in the literature. These aq. QDs were prepared in a simple, safe and non-expansive one-pot reaction in short times and low temperatures. Although stable, P(AAA) coated QDs are relatively large with poor luminescence. Adaptation of binary coating mixture with 3MPA or cysteine both improved the luminescence and control of the particle size. Nanoparticles with the binary coating had smaller crystal sizes with narrower size distribution and comparable or much better luminescence than corresponding CdS nanoparticles coated with only P(AAA), cysteine or 3MPA. This indicates a synergy originating from using a mixed coating system. P(AAA)-3MPA mixture provided a better control of particle size than P(AAA)-cysteine, meaning particles luminescing in different colors. Highest quantum yield and best stability was achieved by 3MPA-80. Moreover, viability of the cells are excellent upto 0.4 mg/ml dose in HeLa cells.For cysteine and P(AAA) binary coating, best luminescing CdS nanoparticles was achieved at the coating compositions of 60/40 P(AAA)/cysteine and best stability was achieved at the coating compositions of 40/60 P(AAA)/cysteine.

In vitro cell viability of these QDs show that poly (2-acetamidoacrylic acid) is a promising candidate for providing biocompatible, non-toxic coating. In addition, the toxicity of 3MPA can be decreased dramatically when it is used with poly (2-acetamidoacrylic acid) as a binary coating material even at the level of 20%. Cysteine is an advantageous coating for a QD for biological applications because it is biocompatible and non-immunogenic**.** Toxicity of QDs gets worse as the cysteine amount in the coating decreases dramatically. Polymeric coatings usually provide a more stable surface coating which provide a greater colloidal stability but they fail to provide a dense coating on the particle surface, leaving trap sites which is detrimental for luminescent properties. Effective surface passivization can be achieved by the incorporation of small molecule. Therefore, binary coating system enhances not only

the physical properties of the quantum dots but it also provides improvement in the cytotoxicity of the quantum dots.

Appendix 1

[1]H NMR OF POLYMERS

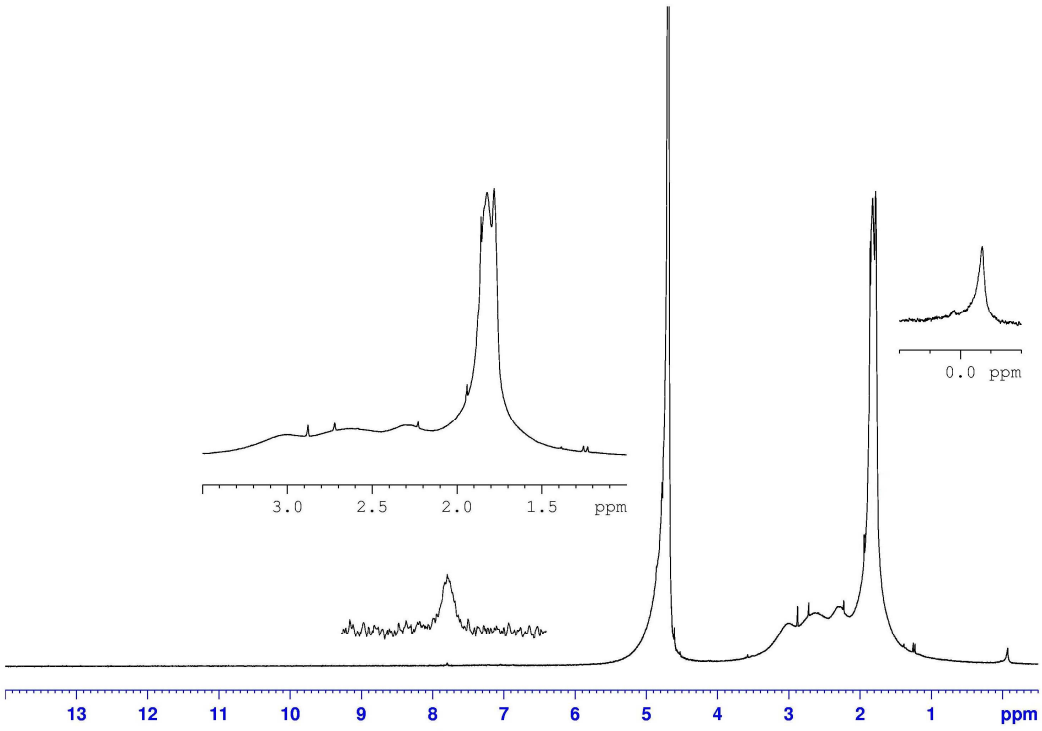

Figure A.1 [1]H NMR (in D_2O)of poly(2-acetamidoacrylic acid).

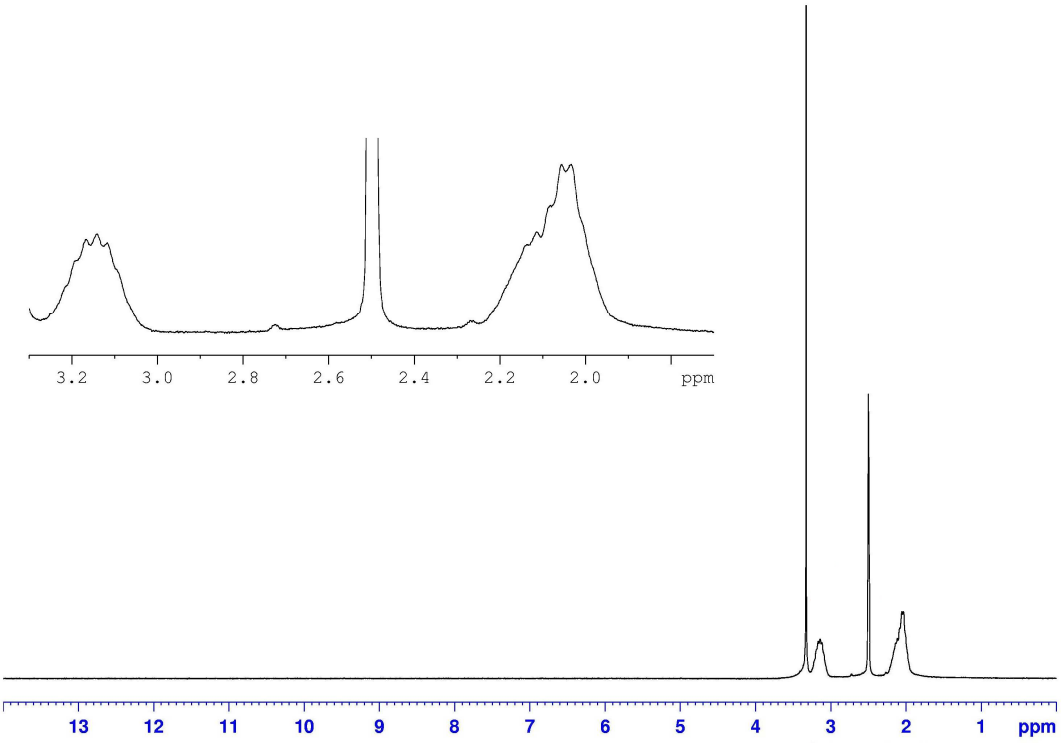

Figure A.2 ^{1}H NMR (in DMSO-d_6)of poly(acrylonitrile).

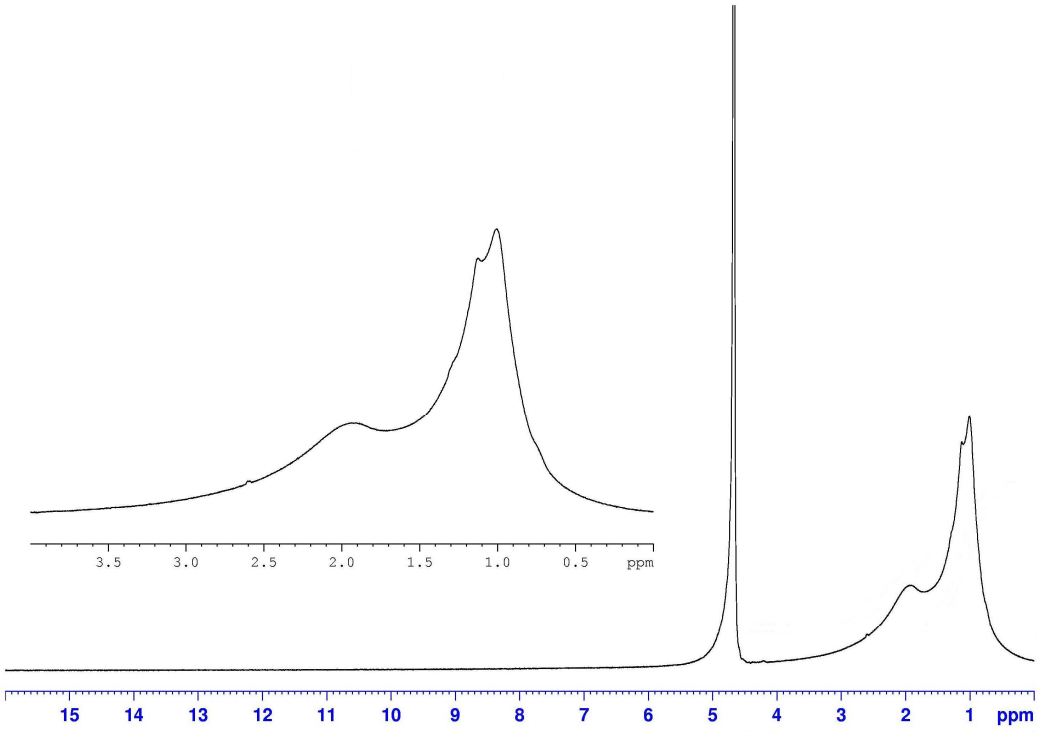

Figure A.3 ^{1}H NMR (in D_2O)of poly(methacrylic acid).

VITA

Yasemin Yar was born in Marmaris, Turkey in 1986. She completed her high school in İzmir in Izmir Turkish Science School (ITK) in 2004. She received her B.S. degree from the Department of Chemistry at Koç University, Istanbul, in 2009. The same year, she started her study M.S. degree in the Department of Materials Science and Engineering at Koç University. Her research interests are colloidal fluorescent and magnetic nanoparticles, rheology of nanoparticle slurries and antibacterial polymers. She will continue her academic career in Polymer Science Ph.D. program at Friedrich Schiller University of Jena, Germany.

BIBLIOGRAPHY

1. Tanaka, H., Recent developments in radical stabilization in polymers and in polymerization. *Progress in Polymer Science* **1992,** 17, (6), 1107-1152.
2. Tanaka, H., The captodative effect in polymer science. *Trends in Polymer Science* **1993,** 1, (11), 361-365.
3. Tanaka, H., Captodative modification in polymer science. *Progress in Polymer Science* **2003,** 1, (28), 1171-1203.
4. Viehe, H.G; Janousek, Z.; Merenyi, R., The captodative effect. *Account of Chemical Research* **1985,** 18, (5), 148-154.
5. Cuthbertson, W.R.; Phillips, H., The action of alkalis on wool: 1. The subdivision of the combined cystine into two fractions differing in their rate and mode of reaction with alkalis. *Biochemical Journal* **1945,** 39, (1), 7-17.
6. Kluskens, L.D.; Kuipers, A.; Rink, R.; de Boef, E.; Fekken, S.; Driessen, A.J.; Kuipers, O.P.; Moll, G.N., W.R.; Phillips, H., Post-translational modification of therapeutic peptides by NisB, the dehydratase of the lantibioatic nisin. *Biochemistry* **2005,** 44, (38), 12827-12834.
7. Süzen, S., The role of dehydroalanines in enzyme and peptide chemistry. *Ankara Ecz. Fak. Derg.* **1999,** 28, (2), 129-141.
8. Jung, G., Lantibiotics-ribosomally synthesized biologically active polypeptides containing sulfide bridges and α,β–Didehydroamino acids. *Angewandte Chemie* **1991,** 30, (9), 1051-1192.
9. Chan, W.C.; Dodd, H.M.; Horn, N.; Maclean, K.; Lian, L.Y.; B.W., Bycroft; Gasson, M.J.; Roberts, G.C., Structure-activity relationships in the peptide antibiotic nisin: role of dehydroalanine 5. *Applied and Environmental Microbiology* **1996,** 62, (8), 2966-2969.
10. Mathias, L.J.; Hermes, R.E., Synthesis and characterization of a novel comb polymer derived from a difunctional monomer: Poly (methyl-2-decanamidopropenoate) [Poly (N-decanoyldehydroalanine methyl ester)]. *Macromolecules* **1986,** 19, (6), 1536-1542.
11. Mathias, L.J.; Hermes, R.E., Polymers from captodative dehydroalanine monomers: 2-Alkanamide derivatives of methyl propenoate. *Macromolecules* **1988,** 21, (1), 11-13.
12. Tanaka, H.; Suzuka, T.; Hada K.; Tezuka, Y., Kinetic study on free radical polymerization of 2-Acetamidoacrylic acid and formation of hydrogel. *Polymer Journal* **2000,** 32, (5), 391-394.
13. Tanaka, H., Control of radical polymerization by captodative stabilization and polarization. *Trends in Polymer Science* **1996,** 4, (4), 106-108.
14. Masuda, S.; Minagawa, K.; Kobayashi, T.; Tanaka M., Polymerization and copolymerization of α-Acetylaminoacrylic acid. *European Polymer Journal* **1998,** 34, (8), 1081-1083.

15. Ha, E.J..; Park, C.H.; An, S.S.; Paik, H.; Lee, J.O., Preparation and characterization of inorganic-organic composites with highly dense CdS nanoparticles using poly(2-acetamidoacrylic acid) hydrogels. *Composite Interfaces* **2009,** 16, (4), 493-505.
16. Masuda, S.; Minagawa, K.; Ogawa, H.; Tanaka, M., Polymerization and copolymerization of α-Acetylaminoacrylate. *European Polymer Journal* **2000,** 201, (14), 1787-1792.
17. Al-Muaikel, N.S.; Al-Diab, S.S.; Al-Salamah, A.A.; Zaid, A.M., Synthesis and characterization of novel organotin monomers and copolymers and their antibacterial activity. *Journal of Applied Polymer Science* **2000,** 77, (4), 740-745
18. Moon, W.S.; Chung, K.H.; Seol, D.J.; Park, E.S.; Shim, J.H.; Kim, M.N.; Yoon, J.S., Antimicrobial effect of monomers and polymers with azole moieties. *Journal of Applied Polymer Science* **2003,** 90, (11), 2933-2937.
19. Drbohlavova, J.; Adam, V.; Kizek, R.; Hubalek, J., Quantum dots-characterization, preparation and usage in biological systems. *International Journal of Molecular Sciences* **2009,** 10, (2), 656-673.
20. Ashby, M.F., Ferreira J.S.G., Schodek D.L. (2009). *Nanomaterials, nanotechnologies and design: an introduction for engineers and architects.* Butterworth-Heinemann: Technology & Engineering
21. Bajaj, P.; Sen, K.; Bahrami, S.H., Solution polymerization of acrylonitrile with vinyl acids in dimethylformamide. *Journal of Applied Polymer Science* **1996,** 59, (10), 1539-1550.
22. Bajaj, P.; Sreekumar, T.V.; Sen, K., Effect of reaction medium on radical copolymerization of acrylonitrile with vinyl acids. *Journal of Applied Polymer Science* **2001,** 79, (9), 1640-1652.
23. Pandey, G.C., Fourier transform infrared microscopy for the determination of the composition of copolymer fibres: acrylic fibres. *Analyst* **1989,** 114, (2), 231-232.
24. Odian G., *Principle of Polymerization,*Wiley Inter-Science, New York, Ch.3 (1981).
25. Blauer, G., Polymerization of methacrylic acid at pH 4 to 11. *Trans. Faraday Soc.* **1959,** 56, (0), 606-612
26. Demas, J.N.; Crosby, G.A., The measurement of photoluminescence quantum yields. *Journal of Physical Chemistry* **1971,** 75, (8), 991-1024
27. Brus, L.E., Electron and electron-hole interactions in small semiconductor crystallites-the size dependence of the lowest excited electronic state. *Journal of Chemical Physics* **1984,** 80, (9), 4403-4409.
28. Acar, H.; Celebi, S.; Serttunali, N.I.; Lieberwirth, I., Development of highly stable and luminescent aqueous CdS quantum dots with poly(acrylic acid)/mercaptoacetic acid binary coating system. *International Journal of Nanoscience and Nanotechnology* **2009,** 9, (5), 2820-2829.
29. Ozturk, S.S.; Selcuk, F.; Acar Yagci, H., Development of color tunable aqueous CdS-Cysteine quantum dots with improved efficiency and investigation of cytotoxicity. *Journal of Nanoscience and Nanotechnology* **2009,** 9, (5), 1-10.

30. Aldana, J.; Wang, A.J.; Peng, X., Photochemical instability of CdSe nanocrystals coated by hydrophilic thiols. *Journal of American Chemical Society* **2001,** 123, (36), 8844-8850.
31. Yu, W.W.; Chang, E.; Drezek, R.; Colvin, V.L., Water-soluble quantum dots for biomedical applications. *Biochemical and Biophysical Research Communications* **2006,** 348, (3), 781-786.
32. Rawlinson, L.B.; Ryan, S.M.; Mantovani, G.; Syrett, J.A.; Haddleton, D.M.; Brayden, D.J., Antibacterial effects of poly(2-(dimethylaminoethyl)methacrylate) against selected gram-positive and gram-negative bacteria. *Biomacromolecules* **2010,** 11, (2), 443-453.